A Comparative Analysis of Single and Modular Proton Exchange Membrane Water Electrolyzers for Green Hydrogen Production- A Case Study in Trois-Rivières

Ashkan Makhsoos*[1], Mohsen Kandidayeni[2], Loïc Boulon[1], Bruno G. Pollet[3]

[1]Institute for Hydrogen Research (IHR), Department of Electrical Engineering and Computer Science, Université du Québec à Trois-Rivières (UQTR), 3351 boulevard des Forges, Trois-Rivières, Québec G9A 5H7, Canada

[2]e-TESC Lab, Department of Electrical and Computer Engineering, Université de Sherbrooke, 2500 boulevard de l'Université, Sherbrooke, Québec J1K 2R1, Canada

[3]GreenH$_2$Lab, Institute for Hydrogen Research (IHR), Department of Chemistry, Biochemistry and Physics, Université du Québec à Trois-Rivières (UQTR), 3351 boulevard des Forges, Trois-Rivières, Québec G9A 5H7, Canada

* Corresponding author.

Ashkan.Makhsoos@uqtr.ca

Abstract

Proton Exchange Membrane Water Electrolyzers demonstrate significant potential for hydrogen production from renewable energy sources. Addressing the inherent intermittency of these sources, a modular design for the electrolyzers emerges as an essential avenue of research. This study delves into potential solutions and strategies for harnessing renewable energy efficiently to fuel these electrolyzers and presents a comparative analysis between single-stack and modular designs based on a hypothetical scenario. Using experimental data, the research projects the hydrogen output derived from solar energy in Trois-Rivières. Machine learning techniques are employed to forecast available energy from photovoltaic panel datasets. A strategic power allocation mechanism is introduced to regulate input current across each electrolyzer, aiming to optimize system performance. Experimental evaluations on a purpose-built test bench validate the conversion efficiency of the electrolyzer. Notably, the results suggest that embracing a modular design can amplify hydrogen production by over 33% annually while concurrently minimizing system degradation.

Keywords: Renewable energy; Hydrogen Production; Modular PEMWE; Energy efficiency; Degradation

1. Introduction

Nowadays, global energy consumption is steadily increasing due to population growth and rising standards of living. In this context, reliance on fossil fuels has resulted in heightened environmental pollution, exacerbated global warming, and numerous other crises. Given these circumstances, the development of renewable energy sources (RESs) appears imperative. Therefore, enhancing the efficiency of production, storage, and transfer of renewable energy is pivotal for harnessing these vital resources. The potential synergy between RES and hydrogen offers a promising avenue towards sustainability. Hydrogen (H_2) can serve as an energy carrier in almost all applications where fossil fuels are currently utilized, such as in automotive and stationary applications, without producing harmful emissions [1]. Thus, giving special attention to H_2 is essential for achieving zero-emission technologies [2]. For example, electrolyzers show promise for H_2 production (HyPro) in renewable energy storage applications. Hassan et al. offer a detailed review of green H2 production technologies, touching upon their technical, economic, ecological, and social facets, and emphasize the pressing research requirements to integrate renewable energy, cut production costs, and fill the void of environmental and techno-economic analyses of renewable H_2 pathways [3].

The proton exchange membrane water electrolyzer (PEMWE) is distinguished from other electrolyzers by its unique characteristics, including high efficiency [4], rapid response [5], flexibility, and scalability[6]. It has also garnered significant interest as an emerging technology for standalone systems in remote locations [7]. Consequently, PEMWEs are being deployed globally, continually setting new benchmarks in capacity and efficiency for the production of green H_2 using clean energy. For instance, the installation of an 8.75-MegaWatt (MW) PEMWE in Wunsiedel, Germany, is projected to cut Carbon Dioxide (CO2) emissions by 13,500 tons [8].

Meanwhile, in Bécancour, Canada, a 20 MW PEMWE generates 8.2 tons of green H2, mitigating the release of approximately 27 thousand tons of CO2 [9]. While PEMWE possesses several advantages as mentioned above, it also comes with certain limitations. These encompass relatively high production costs, shorter lifespans, sensitivity to impurities, and vulnerability to extreme flow frequencies. However, these challenges are actively being addressed through continuous research and development in the field.

PEMWEs have garnered significant attention in both industrial and academic realms. This growing interest is manifested by the burgeoning body of scientific literature and research endeavors aimed at advancing the technology and its applications in green HyPro. Khelfaoui examined the performance of a solar photovoltaic (PV)-PEMWE system for HyPro in the Algerian Sahara region. The study encompasses PV module characterization and validation, as well as the exploration of the effects of ambient temperature and solar radiation on PV performance. The research also evaluates the system's performance under various weather conditions and documents a high HyPro yield of 284 L in a single day [10]. Cai et al. [11] constructed and analyzed a PV system directly coupled to a PEMWE, employing a genetic algorithm to design a working condition boasting 98.8% coupling efficiency. The researchers discovered that fluctuations in PV conditions led to more significant irreversible damage and degradation, attributed to an increased charge transfer impedance (Rct) and ion pollution. Zhang et al. devised a renewable energy utilization model for HyPro and power generation by amalgamating PV, electrolyzer, and fuel cell (FC) modules. The system's efficiency oscillated between 6% and 7% under varying environmental conditions. With a 28 m^2 PV array, the system could produce over 4100 kWh of electricity, satisfying 70% of a household's annual electricity needs, thus showcasing the viability of the PV-electrolyzer-FC configuration for efficient and eco-friendly solar energy harnessing [12].

The application of PEMWE technology has the potential to revolutionize the Power-to-Gas (PtG) process and optimize the use of RES for HyPro. Kotowicz et al. introduce a methodology to ascertain the efficiency of an H2 generator that incorporates a PEMWE, accounting for the power needs of its auxiliary systems. The authors share findings from laboratory experiments conducted on an H2 generator across a spectrum of device loads. They put forward generalized metrics for H2 generator efficiency, applicable in analyzing a PtG system paired with a 40 MW wind farm having a predetermined annual power distribution. A strategy for evaluating the thermodynamic and economic attributes of a PtG setup is presented. The authors further illustrate that the nominal power of H2 generators, the extent of their nominal power utilization, and the economic facets of the PtG setup are all influenced by the level of storage [13, 14].

The intermittent nature of renewable energy sources poses challenges in the development of various green energy solutions [15]. For example, supplying PEMWE with fluctuating power stemming from the variable behavior of RES can lead to degradation and corrosion, which notably shortens its lifespan [16]. Razzhivin et al. suggest the employment of synthetic inertia for wind power plants. This aims to enhance the dynamic stability of the power system and, by extension, the wind energy H2 system through tuning the parameters of the synthetic inertia [17]. Frensch et al. have delved into PEMWE performance and degradation under seven distinct operating conditions [18]. Their research indicates that the dynamic operation of electrolysis accelerates the deactivation rate of the catalyst. Moreover, the efficiency of electrolysis is intrinsically linked to input power and current

[19]. As a result, the electrical power supply process of PEMWE warrants particular consideration [20].

Numerous solutions have been advanced by experts from varied backgrounds and domains to address the unpredictability and inconsistency of renewable energies. Honsho et al. assess the resilience of a PEMWE cell against wind power voltage variations. They formulated an accelerated potential fluctuation test protocol, drawing on wind power voltage fluctuations spanning a 24-hour period. The findings suggest that both reversible and irreversible losses resulting from the degradation of anode catalyst layers can be mitigated by incorporating rest intervals during operation [21]. Various approaches to these solutions can be pursued either individually or synergistically. Addressing these challenges can occur at multiple stages, such as at the power source, during the processing of incoming electricity, and throughout the electrolysis phase. Figure 1 offers a schematic representation of potential strategies to counteract the detrimental impacts of renewable energy at different stages. From this illustration, it is evident that the obstacles tied to using RES for PEMWE can be tackled in multiple ways. Proposals encompass hybrid energy sources, power conversion and control strategies, forecast and optimization using machine learning (ML) algorithms, and flexible, multi-functional structures. Importantly, contemporary HyPro systems frequently merge these techniques at varying phases. The choice of suitable solutions for a venture depends on regional geography, existing resources and infrastructure, potential, logistical considerations, and financial limitations. Continued research, such as delving into modular PEMWE and predictive RES models, is crucial for crafting more proficient and dependable HyPro frameworks. Despite burgeoning interest, a pronounced research gap persists, primarily concerning predicting available energy for green HyPro in PEMWE setups powered by RESs. This uncertainty complicates assessments of this technology's sustainable HyPro potential. This research, therefore, endeavors to bridge this lacuna by probing the feasibility of utilizing ML to predict the efficacy of solar power-driven PEMWE systems, bolstering green and efficient HyPro. A comparative review of modular versus standalone PEMWE systems is vital to gauge their performance and delineate their respective pros and cons. The absence of such juxtapositions in current literature is striking. Such analysis can shed light on efficiency, longevity, cost-benefit, and scalability — all pivotal for the widespread adoption of PEMWE systems. Consequently, a thorough exploration of the performance metrics of both modular and standalone PEMWE units can substantially aid the evolution of enhanced and sustainable HyPro solutions.

Given the topics previously addressed, this study offers insights into potential solutions for challenges associated with the coupling of RESs and PEMWE systems for HyPro. Specifically, we delve into the advantages of deploying a modular PEMWE configuration in contrast to a singular stack system. The central objective is to assess the viability of facilitating green and efficient HyPro in Trois-Rivières by leveraging RESs. To gauge the practicality of RESs for HyPro, meteorological data alongside solar energy readings from Trois-Rivières are gathered. Subsequently, an artificial neural network (ANN) is utilized to project future energy viability. Drawing on this data, we conceive an experimental PEMWE blueprint for HyPro that aligns with the observed renewable energy trends. The projections for the PEMWE HyPro model are informed by the available energy data and prevailing operating conditions. Preliminary findings suggest that transitioning to a modular PEMWE design can notably augment HyPro while simultaneously diminishing degradation and wear, particularly when juxtaposed with traditional singular stack configurations.

The subsequent sections of this paper are structured as follows: Section 2 encapsulates a succinct literature review on existing solutions pertinent to the complexities of harnessing RESs for PEMWE operations. Section 3 outlines a comparative analysis of H2 production employing both singular stack and modular PEMWE setups. Section 4 showcases the garnered results, and Section 5 draws the paper to its conclusion.

2. Possible solutions to the challenges of using RES for PEMWE

Figure 1a illustrates that by utilizing multiple RESs or integrating RESs with other energy sources, enhanced power and diversity in the electrolyzer power supply can be achieved. This solution encompasses increasing the capacity of the power plant, adding different types of energy sources, and incorporating batteries [22] or supercapacitors [23] for backup. The second stage, depicted in Fig. 1b, involves powering the electrolyzer with processed electricity and transferring it from the source to its input. In this stage, converters, regulators, and electrical controllers play a significant role [24, 25].

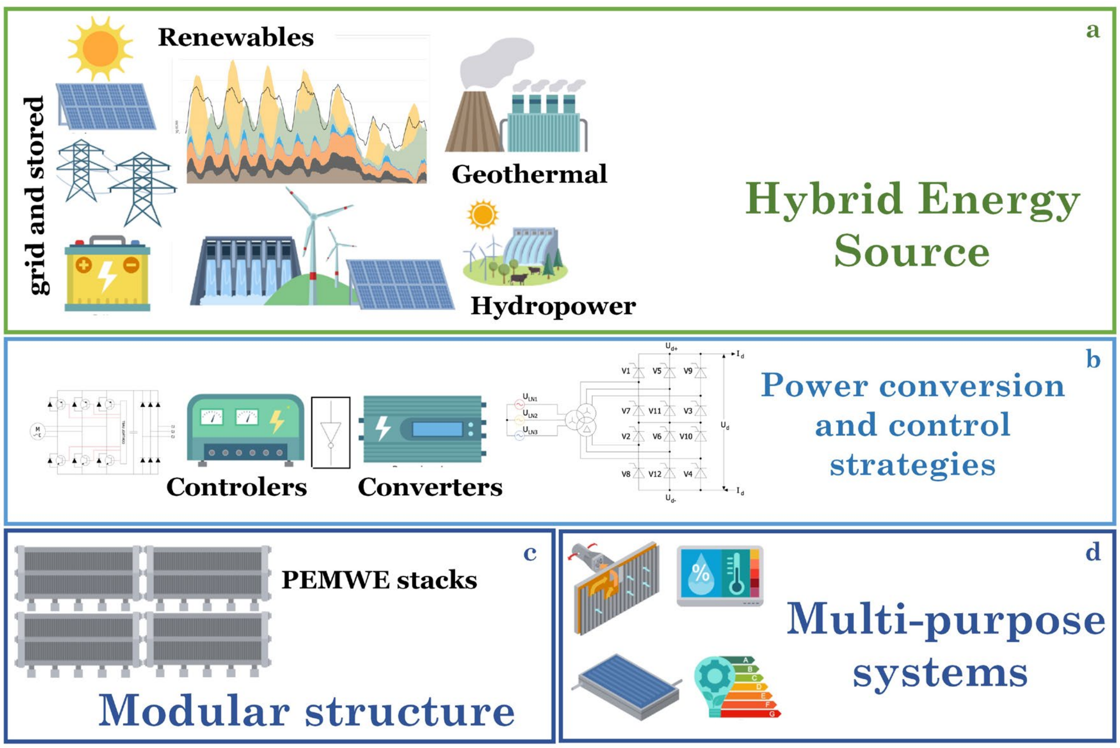

Figure 1 Frameworks for applying possible solutions to RES utilization challenges in PEMWE

The third stage, depicted in Figure 1, addresses the effects of fluctuations and the periodicity of renewable energy. This stage involves the system's structure and complexity, in which the electrolyzer may be a component. PEMWE's modular structure stands out due to its capability to incorporate various features such as power sharing, conversion, and energy management. Power sharing or energy management can entail mechanisms, switches, or controls that utilize the appropriate amount of power at the right moments to enhance the overall efficiency of the electrolyzers, ensuring they are not subjected to high currents and voltages that could harm them. An example of this approach includes power allocation and optimal switching control strategies among system components [26]. Employing hybrid or multi-purpose systems also proves beneficial for this objective, as they stabilize input power for electrolysis [27, 28].

2.1.Hybrid energy source

Using multiple energy sources can yield continuous electricity. The concept of utilizing various energy sources to provide uninterrupted electricity isn't novel. However, it gains significance with RES [29]. Given the intermittent and irregular nature of RESs, there is a general need for a consistent electricity supply. Thus, the interplay of various RESs to achieve relative sustainability is intriguing, and substantial progress has been made in this area [30].

For instance, a case study in [31] elucidates how renewable energy sources can complement each other in Brazil. Figure 2 illustrates the complementarity between solar and wind energy, particularly from mid-spring to late autumn. The figure also highlights how solar and wind energies can offset hydropower's deficiencies during the latter half of the year. The averaged graph indicates that the synergy among these energy sources results in relatively consistent production year-round. Globally, various RESs can be combined to yield a reasonably stable and reliable energy output. Additional RESs, like geothermal, wave, and tidal energies, can be incorporated. Li et al. [32] explored multi-energy HyPro systems and termed them "multi-energy complements." Consequently, multi-energy H2 complementary systems can draw from a plethora of renewable sources, including solar, hydro, wind, tidal, biomass, and others. Kojima et al. [33] postulate that large-scale PV and wind power plants, which benefit from smoothing effects, could be a primary solution to RES challenges. A study by Serdar Genç et al. on wind energy conversion systems (WECS) exemplifies how RES power plants might cater to PEMWEs [34]. Zaik & Werle [35], after a mini-review of RESs as PEMWE energy sources, assessed an electrolyzer paired with solar panels and wind turbines. Their findings suggest that wind and solar energies can compensate for each other's seasonal shortfalls. Moreover, utilizing a buffer battery allows the system to harness the optimal energy amount, preventing overcharging or activation losses.

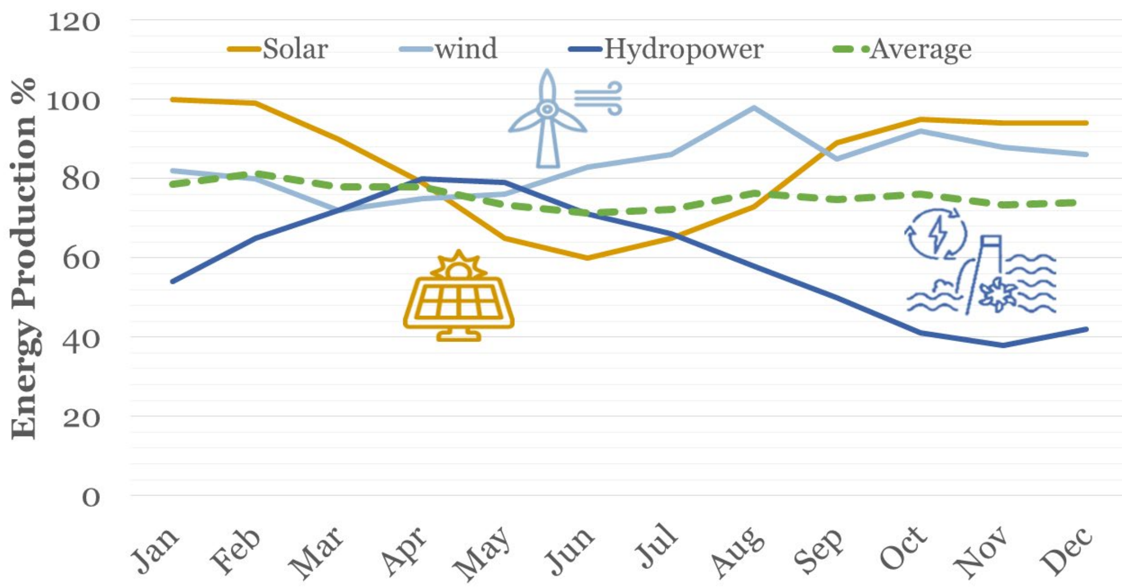

Figure 2 A case of complementarity of RES [31]

In scenarios where one or multiple power sources function erratically, batteries typically serve as storage units to ensure consistent voltage. Stand-alone renewable energy systems aptly illustrate this application [36]. In certain systems, supercapacitors can assume a similar role [37]. Conversely, when there is a surplus of renewable energy, it can either be fed into the grid or used by other systems via the multidirectional H2 conversion system [38]. This not only protects PEMWE from potential damage due to excess electricity but also facilitates its effective utilization or storage. Koponen et al. [39] evaluated PEMWE's performance in the context of RES. They analyzed dynamic functional properties and operational constraints from a renewable energy standpoint, suggesting supercapacitors or batteries for uninterrupted electrolysis based on a ten-hour test with a 1 Nm3/h PEMWE powered by a 5 kW solar PV. They concluded that the peak HyPro in a PEMWE system, without separate post-electrolysis compression, is achieved when the H2 outlet pressure closely aligns with storage pressure.

2.2.Power conversion and control strategies

Scaling up and enhancing PEMWE to the MW scale poses substantial challenges for both the existing components and the power management of the input. PEMWE input power managers encompass appropriate source selection, power allocation, control of power fluctuations, start-stop switching [40, 41], power conversion [42], and prolonged high-power operation (Figure 1.b).

From the electrical perspective described in the prior section, the WECS highlighted the pivotal role of converters in the optimal power delivery to the PEMWE. For hydrogen generation from deionized water, electrolyzers necessitate a very low DC voltage, prompting the common use of step-down converters [43]. Yodwong et al. examined the AC-DC converters currently employed for power transmission from renewable energy conversion systems and the grid for both PEMWE and alkaline electrolyzers. Their research primarily addressed converters centered on thyristor rectifier bridges and chopper-rectifiers [24]. They probed into challenges concerning specific energy consumption, current ripple, reliability, efficiency, and power quality associated with these converters. While the application of thyristor-based rectifiers in high-power contexts has been showcased, the integration of active and passive filters becomes imperative to elevate power quality. Their findings also indicated that amalgamating a chopper with a rectifier can boost power quality by eliminating the need for sizable active and passive filters. Nonetheless, employing a basic chopper (buck converter) is not devoid of downsides, especially in terms of reliability, energy efficiency, voltage ratio, and current ripple. To counteract these pressing challenges and uphold the sustainability of HyPro, the deployment of novel DC-DC converters aligned with the emergence of new power sources is essential. As per Wang et al. [44], a solar energy-driven fast charging and HyPro system can be regulated through a semi-decentralized control strategy for a DC microgrid. This undertaking segregates the PEMWE energy control into decentralized and power-based modes, with the PEMWE controller dictating the system mode by referencing the day's lowest network cost. Similarly, Gu et al. crafted a system marrying PV power generation with proton exchange membrane water electrolysis for green HyPro. They proposed an energy management strategy to ensure consistent HyPro throughout the day and enhance energy utilization efficiency. Validated via Matlab/Simulink-based simulation, the results underscored that integrating a battery for energy storage markedly uplifts the system's energy efficiency and trims the light discard rate [45]. Moreover, Vudata et al. unveiled a multi-software power control approach built on an electrochemical dynamic stack model. This model delineates the potency of electrolyzers in tempering PV signals to bolster grid stability and adaptability. Alongside highlighting HyPro and electrolyzer efficacy, the study also offers insights on electrolyzer sizing as a tactic to curtail short-lived power surges prompted by cloud cover [46]. Finally, Crespi et al. examined a 60 kW PEMWE setup to introduce a dynamic model for a large-scale PEM electrolysis system, delving into its adaptability during inconsistent and partial load operations. Experimental validation affirmed the model's forecasts with a deviation of less than 4%, pinpointing an elevated specific consumption at diminished current densities. The investigation inferred that this performance decrement predominantly stems from the conventional plant control methodology, power uptake of auxiliaries, and hydrogen utilization for dryer rejuvenation. The implementation of astute control strategies, like modulating the water flow rate and PSA columns' rejuvenation, slashed the net specific consumption by 21% and 50%, respectively [47].

2.3. Prediction and Optimization of PEMWE with machine learning

Using Machine Learning (ML) algorithms in engineering modeling for HyPro can facilitate the optimization and study of key components and materials in PEMWE. This can substantially reduce the associated costs and expedite the conventional trial-and-error multivariate experimental optimization process [48]. Günay & Tapan employed ML techniques to explore the connection between descriptor variables and outputs in PEMWE, pinpointing the influence of particular materials and operational characteristics on current density, power density, and polarization. Their findings indicate that ML methodologies can assist in identifying optimal conditions for the design of a PEMWE for HyPro. Moreover, the Bayesian optimization algorithm can achieve peak performance more efficiently in terms of time and effort compared to traditional research methods [49]. Additionally, ML-based simulation models can predict the HyPro rate and cell current density for PEMWE cells given varying design parameters [50]. Salari et al. highlighted the optimization of a solar-based PEMWE utilizing machine learning and animal-inspired algorithms. They achieved a maximum HyPro rate of 5.44 mol h^{-1} m^{-2} and identified solar radiation as the most significant determinant of the HyPro rate. This was followed by factors such as ambient temperature, inlet temperature, working fluid mass flow rate, and wind speed [51]. Meanwhile, Hai et al. delved into a solar-geothermal energy system comprising three turbines for power generation, a PEM electrolyzer for HyPro, and a thermoelectric module for converting excess heat into electricity. This system is capable of generating 3.8 MW of electricity and producing 8 g of H2 fuel per second at the operational point. To optimize design parameters, ML methods were implemented, and the optimal operating point for maximizing power and stored fuel flow rate was ascertained using a genetic algorithm. Their results revealed that the total power output at this optimal point would exceed the standard operational point by approximately 500 kW. Moreover, the H_2 production rate was projected to be nearly 29 g per second at this optimized juncture [52].

2.4.Modular and Multipurpose structures

Beyond the points discussed in the previous subsection, the adaptability of electrolyzers to renewable energy can be enhanced through modifications in their structural design (as depicted in Figure 1.b). This section aims to delve into how modular and multipurpose structures assist various systems in addressing their constraints. Insights from modular energy systems (MES) can offer invaluable guidance for PEMWEs, enabling them to refine existing configurations by leveraging the merits and drawbacks of MES. Illustratively, an MES consists of several autonomous power sources capable of collective operation. In such a system, power distribution spans across components and/or energy storage is apportioned into multiple standardized modules, paving the way for a plethora of economic and technical benefits [53].

Employing MES can bolster the overall system efficiency, especially pertinent in high-power scenarios where the power supply might not perpetually function at its peak efficiency. Figure 3 illustrates that while each module exhibits a unique efficiency, the cumulative efficiency of the modular system (B) surpasses that of individual modules. Contrasted with a single-stack FC, a modular hybrid system encompasses numerous optimal operational points. The right side of the figure (B) plots the efficiency curves for four distinct power sources, ranging from M1 to M4, equipping the system to operate at consistently high efficiency levels. Owing to this characteristic, MESs grant increased operational flexibility, presenting superior power distribution choices across diverse load scenarios.

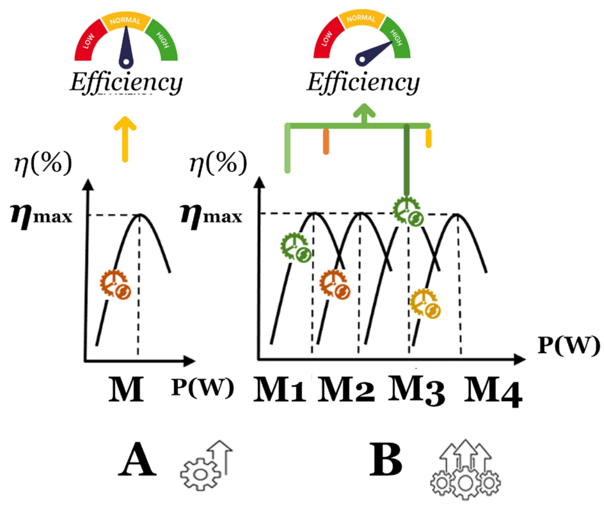

Figure 3 . Efficiency curves of single (A) and modular (B) resources [53]

Moreover, the availability and durability of modular systems can be enhanced through diligent performance monitoring and management. Such systems can also offer redundancy, ensuring continued operation even if one component fails. By identifying each component and efficiently delegating tasks, the system's lifespan and responsiveness are augmented [54, 55]. Another durability enhancer is that the MES components, like FCs and batteries, typically operate at their optimal efficiency levels to deliver peak power. Thus, if lesser power is needed, a single module or a few can function independently, sparing unused modules from wear and tear, extending system longevity.

Architectural flexibility is a further merit of MES, crucial for ensuring system stability and safety. Modular setups offer a plethora of design avenues, allowing for innovative control strategies [56].

A standout advantage of MES is the capability to amplify capacity, bound only by the constraints of the infrastructure, due to the repetitive nature of the modules. However, the capital expense of a modular system might surpass that of a comparable MES with identical power, due to the distinct components. Nonetheless, replacing a low-power component is substantially cheaper than its high-power counterpart. Plus, modular systems stand to benefit from economies of scale.

To expedite the progression of PEM electrolyzers, insights from PEMFCs—which share analogous structure, materials, and processes—can be invaluable. Notably, the evolution of modular FC systems has been a focal point of extensive research [57-61]. Literature posits that modular FC systems, fashioned either by amalgamating multiple stacks or by segmenting a single one, hold promise for the future. These FCs have been devised with diverse electrical and fluidic designs, with their performance contingent on these frameworks. System reliability in a degraded mode is also influenced by its architecture. Moreover, select designs facilitate individual stack control to enhance power output. Depending on the architecture employed, a more robust system can be realized by integrating degraded mode functionality. The insights derived from modular FCs can significantly inform the management of input energy for electrolyzers, given the striking similarities between the study of modular FCs and electrolyzers [62].

2.5. Modular PEMWE

Generally, Modular structures for electrolyzers can generally be categorized into three groups: Multi-electrolyzers [63], segmented electrolyzers [64], and modular electrolyzers. Transitioning from single to modular electrolyzers provides technical and productivity enhancements, along with notable cost savings in HyPro [65]. Depending on system constraints and advantages, various architectural designs may be employed. Table 1 presents several modular designs for PEMWEs. An overview of the essential steps in designing and determining modular PEMWE architecture systems is depicted in Figure 4.

Given that PEMWEs typically harness surplus energy from one or multiple sources, or from Renewable Energy Sources (RES) where input energy can fluctuate considerably, the potential input energy significantly shapes the design of modular PEMWEs. For optimal system efficiency, it is imperative to understand the peak input power and the specific average power rate. Subsequently, other relevant parameters should be factored in when deciding on the type, size, and quantity of stacks.

Three critical areas must be extensively evaluated in subsequent steps: gas, water, and electricity architectures. Decisions regarding gas architecture encompass gas transfer and storage, potential water separators or dryers, the dimensions of H2 tanks, and possibly H2 compression. For water architecture, choices revolve around storage tank specifications and the temperature of the water before it enters the electrolyzer, which may necessitate a preheater. Since the water supply must be deionized, additional considerations might be essential for system design. Lastly, considerations related to electricity architecture involve the power allocation pattern, power conversion framework, and potential control strategies for the system's input power.

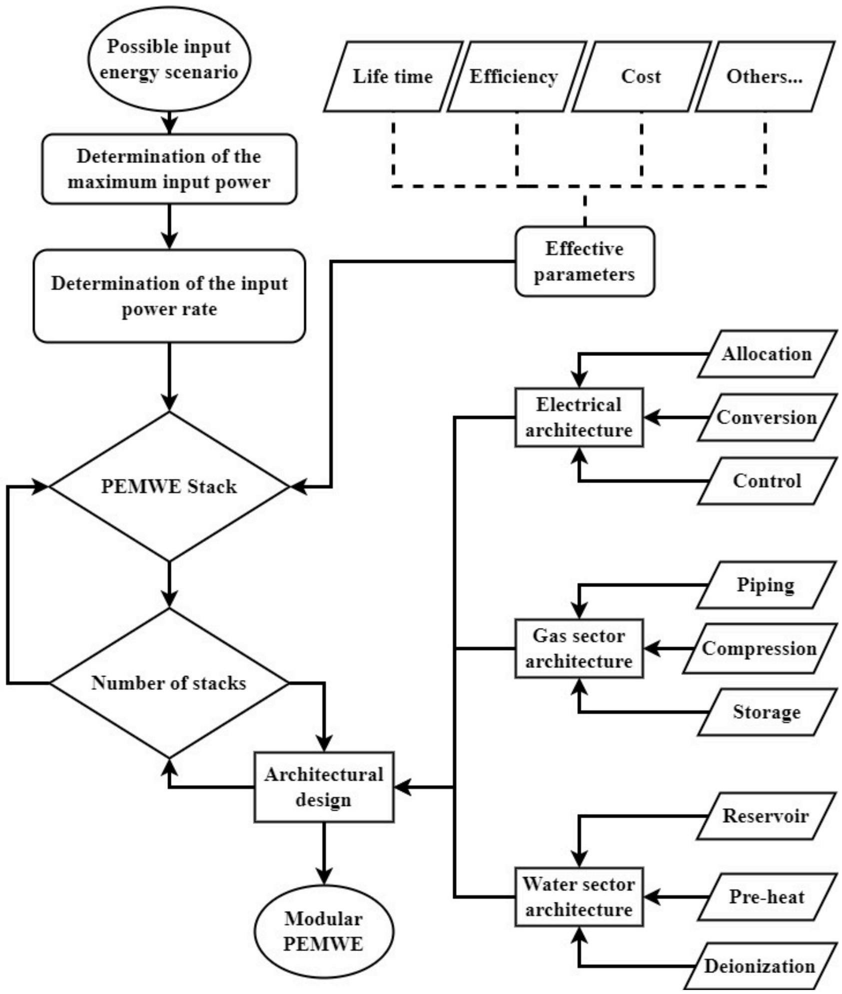

Figure 4 Schematic of PEMWE modular design

Table 1 Successful examples of modular structure in PEMWE

Reference	Modularity (Strategy)	Superiority and creativity	Schematic
[66]	Modular direct coupling with PV (With optimization calculations)	• higher HyPro efficiency • more leakage resistance • No converter • Compact	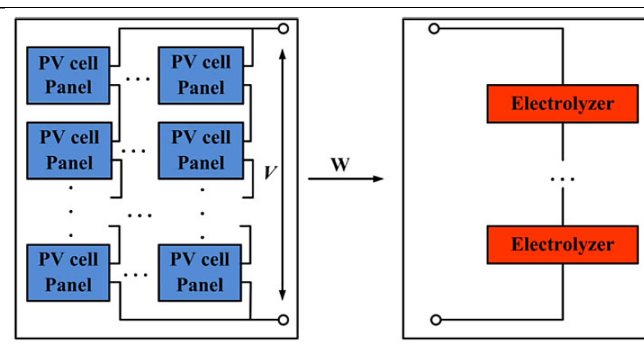

[11]	Single-stack direct coupling with PV (With optimization calculations)	• No need for electrical converters • More compact • Less connections	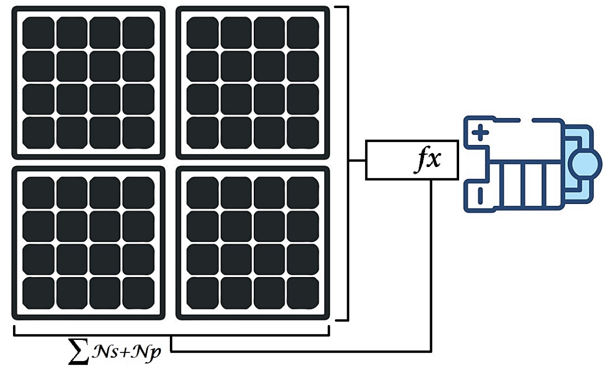
[67]	Modular (Control and conversion)	• Eliminating the intermittency of input energy • Faster dynamic behavior than the wind turbine • Avoiding overvoltage during transients • The operation of each converter in the mode of maximum efficiency	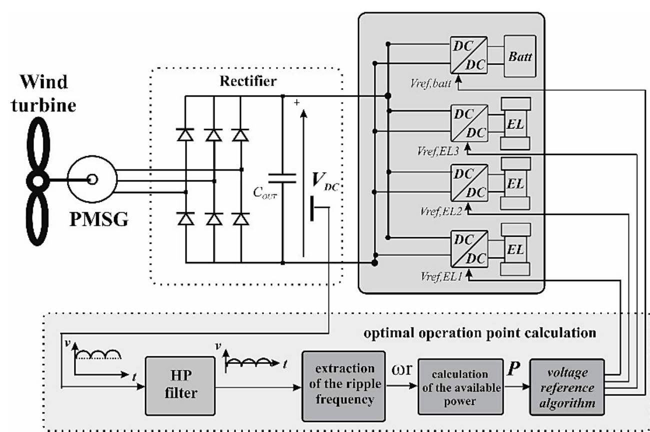

[68]	Modular (Power allocation Optimization)	• PEMWE Maximum efficiency • Lower degradation • Shortened control transient time	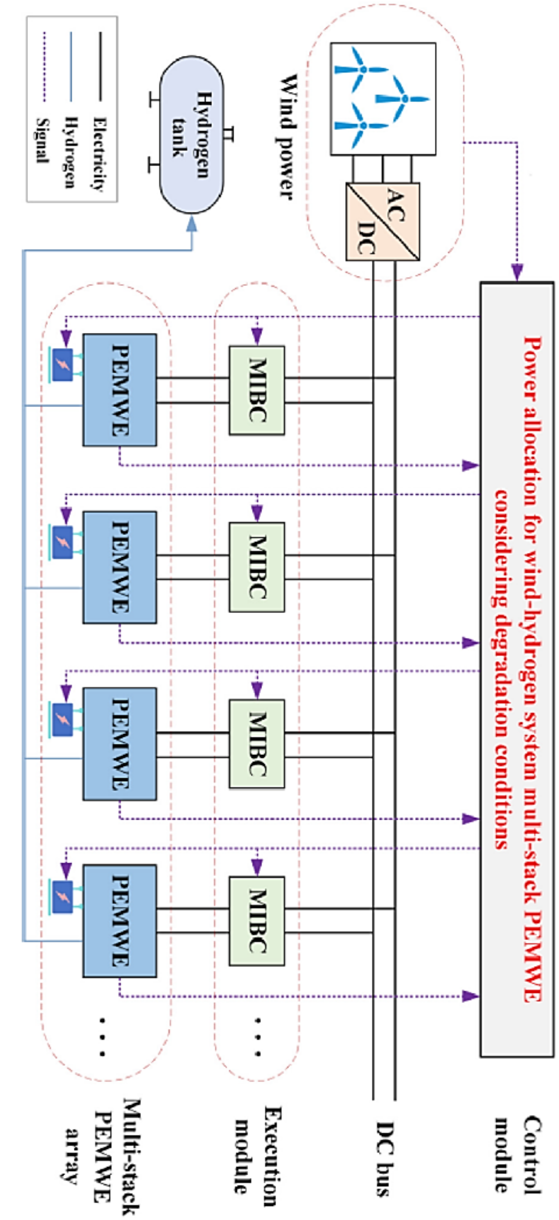

[69]	Multistack (flexible pocket)	• Dynamic high-pressure HyPro • Compact structure and easy stack adjustment and size upgrade • Improved heat management • Direct current and media conduction • Full flexibility	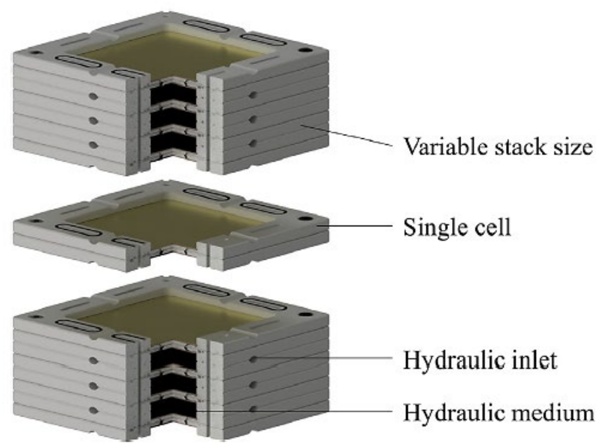

Wirkert et al. [69] introduced a novel modular PEMWE termed "multistack." This design operates uniformly and boasts an efficient heat management system. In their research, a flexible container was fashioned for internal cell components by combining monopolar flat plates with plastic frames. Beyond enhancing heat management and media transfer, this fully modular stack design also presents a more compact form and straightforward stack size adjustments in comparison to traditional models. The capability of this new design for high-efficiency operation, dynamic high-pressure HyPro, and heat management that is independent of process water, has been experimentally validated.

Guilbert & Vitale [67] delved into two primary concerns associated with electrolysis' specific energy consumption: Faradaic efficiency and converter design. To address these issues, they explored a modular setup of PEMWE powered by a wind turbine conversion system. Stacking DC-DC buck converters is employed both for the electrolyzers and wind turbine conversion systems to mitigate ripple and sustain reliability. This converter is orchestrated in a manner that enables faster dynamic behavior than the wind turbine, thereby averting transient overvoltages that could harm the PEMWE. The wind turbine's output power is synchronized with the 400 watts-rated power of the PEMWE. In their energy management strategy, if the power surpasses 400 watts, the electrolyzer operates at its rated power, and the excess power is channeled to the next unit, as depicted in Figure 5. This sequence persists until three electrolyzers are engaged. In particular scenarios where energy production exceeds 1200 watts, a battery is also activated. Figure 5's vertical graph displays the output power in watts every half hour (H/2). The four sections, differentiated by varying shades of green, denote the operating regions corresponding to the number of activated electrolyzers. These regions expand with the augmentation of input energy.

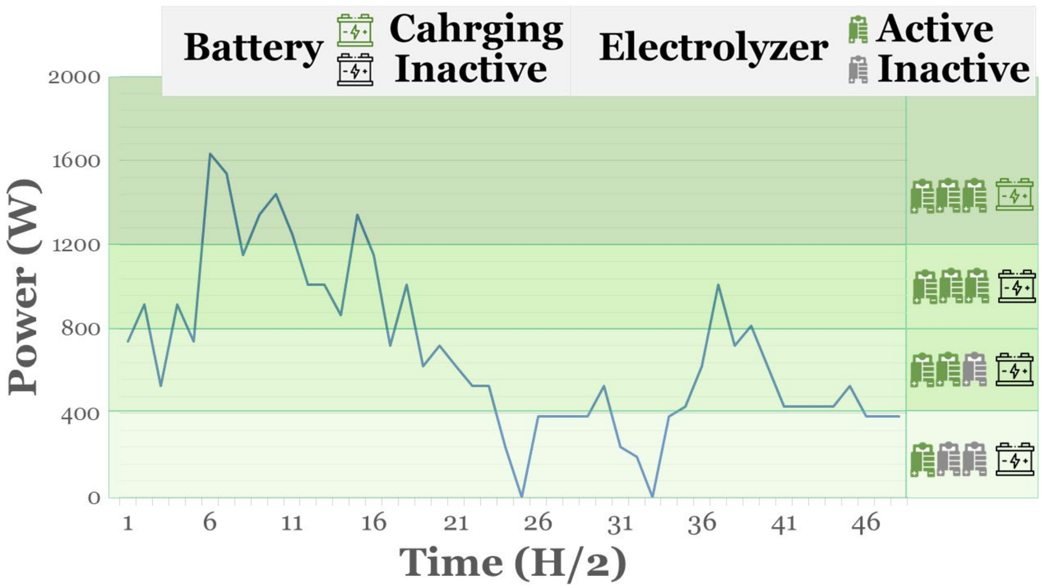

Figure 5 Power-sharing strategy according to the available power from the wind turbine

The architecture of the wind system for HyPro in the research by Lu et al. [68] differs. In their setup, wind power input is paralleled to the modular PEMWE array through a DC bus, and the power allocation is managed by the control module. When power allocation information for each PEMWE stack is gathered, the execution module sends the power allocation signal to the control module. This control module, which governs each PEMWE stack, will also manage the start-stop function during power outages when an external power supply isn't available. Owing to the power allocation control module, the wind H2 system achieves a cumulative energy efficiency of 61.65%, comparable to a power allocation strategy prioritizing optimal efficiency. Using a genetic algorithm method, Cai et al. [11] optimized the coupling parameters between PV and PEM electrolyzers, observing variable conditions when directly coupled.

The advantages of employing a modular structure in sizable HyPro applications become more evident. One key benefit is the ability to replace a production part if it degrades to a point where it is no longer advantageous to maintain within the system. Conversely, degradation occurs when a PEMWE stack is in operation. By restricting the activity of a segment of the system, degradation in that segment is reduced. Thus, a modular structure curtails the rate of degradation both in individual stacks and across the entire system. Figure 6 highlights the pronounced impact of degradation on efficiency and demonstrates how a modular setup can mitigate it. Figure 6.a illustrates that by implementing a power allocation strategy, only some of the PEMWE stacks operate concurrently, significantly reducing degradation. If all PEMWE stacks were active simultaneously, all degradation curves would look alike, with heightened degradation observed in the 2nd, 3rd, and 4th PEMWEs. As seen in Figure 6,b, the efficiency of an electrolyzer diminishes markedly as it degrades. In this instance, there is roughly a 7% efficiency difference between a fully functional stack and one degraded by 0.2-V [68].

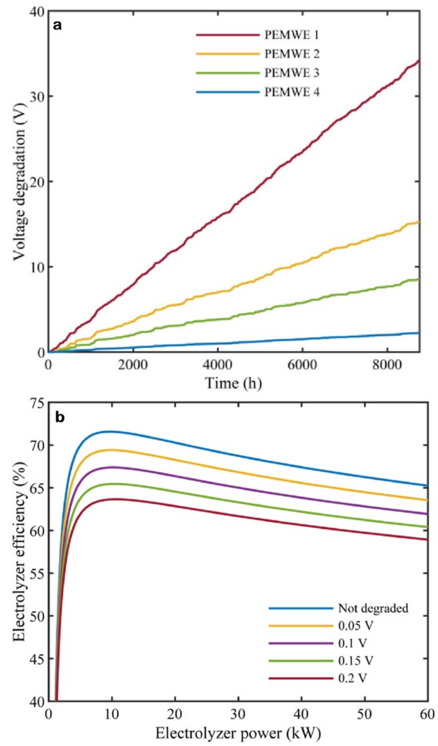

Figure 6 Comparision of degradation in Modular and single-stack PEMWE [68]

2.6. Multi-purpose systems and Combination of Different Strategies

Intermittent effects of RES can be alleviated through hybrid or multi-objective systems, occasionally with a combination of input sources, multiple processes, tasks, or both. Alirahimi et al. delved into a solar thermal power plant integrated with PEMWE for co-generating power, H2, Oxygen (O2), and hot water. Their proposed system yields 2.906 kg of H2 per hour. A thermoelectric generator, used to draw off heat from the Organic Rankine Cycles (ORC) condenser, supplies the PEMWE with additional electricity, as depicted in Figure 2-A. [70]. They also explored a hybrid source multi-objective design powered by geothermal and solar energy. This design employs an ORC and Parabolic Trough (solar) Collectors (PTCs) to generate H2 with PEMWE, achieve water desalination, and also facilitate an absorption cooling system, as illustrated in Figure 2-B [71]. To enhance HyPro, they utilized the steam generator's waste heat to pre-heat the PEMWE's deionized water. Pirom & Srisiriwat [72] integrated PEMWE and PEMFC with a PV array for a residential house, achieving a system efficiency ranging from 1.75% to 7.66%. Such net-zero emission residential houses also have freshwater as a byproduct of PEMFC. Dong et al. assessed a renewable generation system integrating a solar-geothermal driven PEM electrolyzer with ORC, ERC, and RO subsystems. Their analysis spanned energetic, exergetic, economic, and exergoeconomic aspects, optimizing the system with multi-criteria decision making and the Gray Wolf Optimizer technique [73]. Escobedo et al. outlined the design, construction, and performance assessment of a PEMWE, characterized by computational fluid dynamic analysis, CNC milling, and electrospray deposition of electrocatalysts. This system achieved a peak efficiency of 59.65% and a HyPro rate of 42 $NL \cdot h^{-1}$ at 15 V and 70 °C with a 132 Wh power draw [74]. Hasani et al. examined the thermoeconomic feasibility of a renewable production unit. This unit combined a geothermal-based PEMWE with the ORC. Their optimization focused on NPV, cost rate, exergy efficiency, and HyPro rate employing techniques like LINMAP, TOPSIS, Shannon Entropy, VIKOR decision-making, and Gray Wolf Optimizer. Their findings indicated an optimum payback period of 5.07 years and a total destruction of 599.13 kW achievable with ORC/IHE-PEM operating with R113. This setup yielded optimal rates: a cost rate of 26.32 $/hr, HyPro rate of 4.202 kg/h, and an exergy efficiency of 40.66% [75].

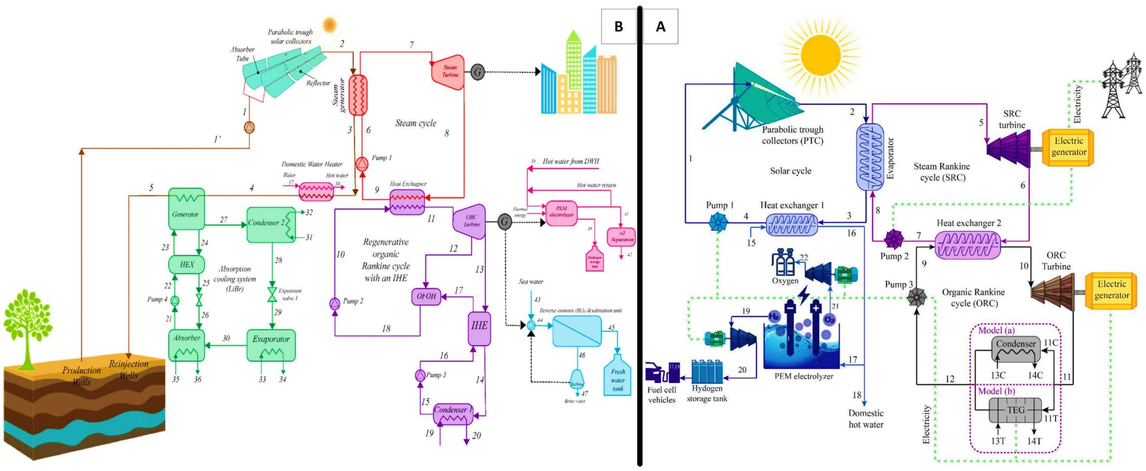

Figure 7 The Multi-objective design for multi-generation energy systems based on renewable sources

Sun et al. present a non-dimensional model of a renewable generation system that integrates a solar-geothermal driven PEMWE with the Kalina cycle, single-effect absorption refrigeration cycle, and RO unit. This system was optimized using response surface methodology, resulting in a unit cost of products of 1.75 $/GJ and an exergetic efficiency of 31.71% [76]. Seyedmatin et al. propose a new cooling cycle for a scramjet designed for co-production of electricity and H2 via a PEMWE. They conducted energetic and exergetic analyses to gauge the system's performance and the ramifications of multi-expansion. Their results indicated that the PEMWE experienced the highest exergy destruction ratio. Multi-expansion systems offered significant benefits over single-expansion systems in terms of electricity, cooling, and HyPro. Additionally, increasing the pump's back pressure yielded more electricity and HyPro, and as the freestream Mach number increased, so did the power, H2 production, and cooling load capacity [77].

Ahmadi Boyaghchi et al. introduce a multi-generation system integrating a dual ORC, biomass gasification, and a PEMWE to produce syngas, power, refrigeration effect, heating load, H2, and O2. Their optimization showed that using R600-R290 as the organic working fluid group resulted in maximum energy and exergy efficiencies of 79.35% and 67.64%, respectively. Additionally, they achieved the minimum total product cost and environmental impact rates of 152.7% and 485.1 Pts/h, respectively [78].

Mohammadi et al. put forth a novel combined biomass-driven cogeneration system comprising a PEMFC and a dual-ejector organic flash cycle. This system aimed to generate clean power while recovering waste heat. It was assessed technologically, economically, and environmentally, with a two-criteria optimization targeting lower costs and emissions alongside higher efficiency. Their findings pinpointed a solution with a net output power of 2.66 MW, a total cost rate of 5.39 $/h, and energy and exergy efficiencies of approximately 37.65% and 23.77%, respectively. They also identified components with the highest exergy destruction, suggesting areas for improvement [79].

Ghorbani et al. crafted an integrated structure for H2 and O2 liquefaction cycles that utilized wind turbines, the Kalina power generation cycle, and electrolyzers. This system could produce 2100 kgmol/h of liquid H2 with specific energy consumption, coefficient of performance, and energy efficiency of 5.462 kWh/kgH2, 0.1384, and 14.06%, respectively. The hybrid system's exergy efficiency stood at 58.73%. Notably, the most significant exergy destruction occurred in electrolyzers (83.13%) and heat exchangers (5.93%) [80].

Yilmaz et al. conducted a thermodynamic evaluation of geothermal energy-powered HyPro via PEM water electrolysis. They found that H2 could be produced at a rate of 0.0340 kg/s with energy and exergy efficiencies of 6.7% and 23.8%, respectively, at a geothermal resource temperature of 160°C. Both efficiencies increased with the electrolysis and geothermal water temperatures [81].

Temiz et al. proposed a unique ocean and solar-based multi-generational system utilizing various renewable sources in a self-sufficient manner. The overall energy and exergy efficiencies were 16.28% and 36.35%, respectively, with the system generating 25.16 GWh of electricity and 283 tons of H2 annually via PEMWE. This system also encompassed a fish farm, greenhouse, and food drying facility, producing 7.9 tons of vegetables and 374 tons of fish annually, presenting a potential remedy for Arctic communities' energy and food challenges [82].

Holmes-Gentle et al. developed a dynamic non-linear process model for a thermally-integrated concentrated PV-electrolysis system. The system exhibited a hysteresis effect in response to perturbations, and the potential for co-generating H2 and heat appeared promising [83].

Zhao et al. formulated an electrolysis power allocation and alternative control method [84], combining an optimized control strategy to forecast the peak wind power at specific times. To stabilize the power output of a wind farm, Muyeen et al. generated a reference for line power, developed a switching strategy, and produced H2 gas to absorb fluctuating wind farm outputs [85].

Shakibi et al. investigated a multi-generation system based on wind turbines and PTCs. This system incorporated a PEMWE for HyPro and utilized an ML-based optimization approach. Their optimal scenario achieved 6.20 MWh of energy and saved 1.26 tons of CO2 per year. Their study also emphasized the influence of parameters like electricity and H2 prices on the system's total cost and exergy efficiency [86].

3. Comparative study of Hydrogen Production

A green HyPro system based on RES demands foresight and meticulous evaluation of two processes to ensure stable, continuous, and reliable production. These processes encompass the assessment of electricity production from renewable sources and the scrutiny of HyPro with the chosen electrolyzer. In Section 3.1, the energy available from the PV array in Trois-Rivieres is evaluated. The experimental data for a PV panel is first gathered. Subsequently, a predictive ANN model is developed using meteorological data and energy production records. This model is then utilized to forecast the amount of energy expected to be available in the future, based on atmospheric conditions and the local climate. Section 3.2 uses the experimental energy production to power a PEMWE stack and assess its performance. In this context, HyPro in Trois-Rivieres is examined by analyzing and scaling the data. Based on the available solar energy, an optimized modular structure is proposed, which is subsequently compared to a conventional system in Section 3.3.

3.1. Available energy

PV energy production largely depends on the array placement, surrounding climate, particulate matter, and industrial emissions. Therefore, detailed and long-term information about a region's weather conditions can enhance the accuracy of energy production forecasts, especially when compared to experiences drawn from a small PV unit. Given sufficient long-term data, ANNs are an invaluable tool for creating reliable predictive models that surpass those generated by current simulations or nominal models. As such, a suitable ANN model, paired with local environmental and climate data, can effectively estimate the solar energy available in Trois-Rivières. As indicated in Eq.(1), the PV output power is predominantly influenced by solar radiation and geographical location; thus, local weather conditions play a significant role [87]. Factors such as cloud cover, atmospheric clarity, temperature, air pressure, and wind are all pivotal parameters that affect the received energy.

$$\mathrm{P}_{\boldsymbol{pv}} = \Upsilon \alpha_{\mathrm{PV}} \mathrm{G}_{\mathrm{nr}}[1 - \mathrm{B}_{\mathrm{r}}(\mathrm{T}_{pv} - T_r)] \tag{1}$$

This formula is typically used to calculate the output power ($\mathrm{P}_{\boldsymbol{pv}}$) of the PV panel. G_{nr} represents solar irradiance, α_{PV} denotes cell efficiency, T_r indicates the operating reference temperature, and B_{r} is the temperature coefficient. Additionally, Υ stands for the surface coverage ratio, which is the module surface area that can be covered by sun irradiation relative to the total area occupied by the array. Solar dynamical positions directly influence Υ, while earth's atmospheric conditions—such as pressure, humidity, atmospheric dust, wind, and transparency—affect G_{nr} directly. Other vital parameters impacting the nominal output power of PV include panel position, soiling, shading, snow, losses, and aging [88].

Given these factors, one of the most accurate methods to determine received solar energy involves collecting experimental data from a PV panel positioned identically as depicted in Figure 7. The University of Quebec in Trois-Rivières presents an ideal site for solar array implementation. The southern face of the university building (Albert-Tessier building) is oriented southward, with a slight 5-degree deviation to the west—optimal for the northern hemisphere. Given the arrays' elevated installation, shading is minimized. Additionally, the window architecture is slightly angled inward, complementing the PV plate's inclination. This setup mitigates several efficiency-reducing factors, including surface shading, snow accumulation (in winter), dust buildup, and high temperatures (in summer). The location also offers convenient access due to the building's windows. These features render this facade suitable for PV array installation, as illustrated in Figure 8. Aesthetically, it enhances the building's appearance. Specifications for the PV panel utilized in the experimental tests are provided in Table 2.

Table 2 The reference PV panel characteristics

Location	Trois-Rivières, Canada
Latitude	46.35° N

Longitude	72.58° W
Module Type	Polycrystalline
Array Type	Fix tilted
Array Azimuth	185°(South-West)
Capacity Factor	12.5%
Array Tilt	66.5°
DC System Size	150 W
Maximum current	8.7 A
Dimensions	149 * 66.5 * 3.5 cm
Number of PV for the estimated array	80
Total effective area of the array	79.268 m2

Data were collected for a year, from 2021 to 2022. Since the PV output is in direct current (DC), it is directly routed to the battery after maximum power point tracking (Figure 6) using a charge controller. Additionally, voltage and current measurements are relayed to the system via an RS-485. This procedure is depicted in Figure 6. Maximum Power Point Tracking (MPPT) is commonly employed to regulate the electrical energy generated by PV arrays. This energy is then channeled to the PEM electrolysis through a DC-DC converter. In this state, the current remains relatively stable. Nonetheless, the high expense of electronic control equipment and efficiency losses due to multiple energy conversions have prompted the exploration of alternative methods. One such method, which can decrease both the number of energy conversions and equipment costs, is direct coupling. This method involves a direct connection between the power source and the electrolyzer. By adjusting the number of solar cells in series and parallel configurations, the system's power level can be kept close to its maximum. Consequently, the HyPro estimation will be grounded on the direct coupling method.

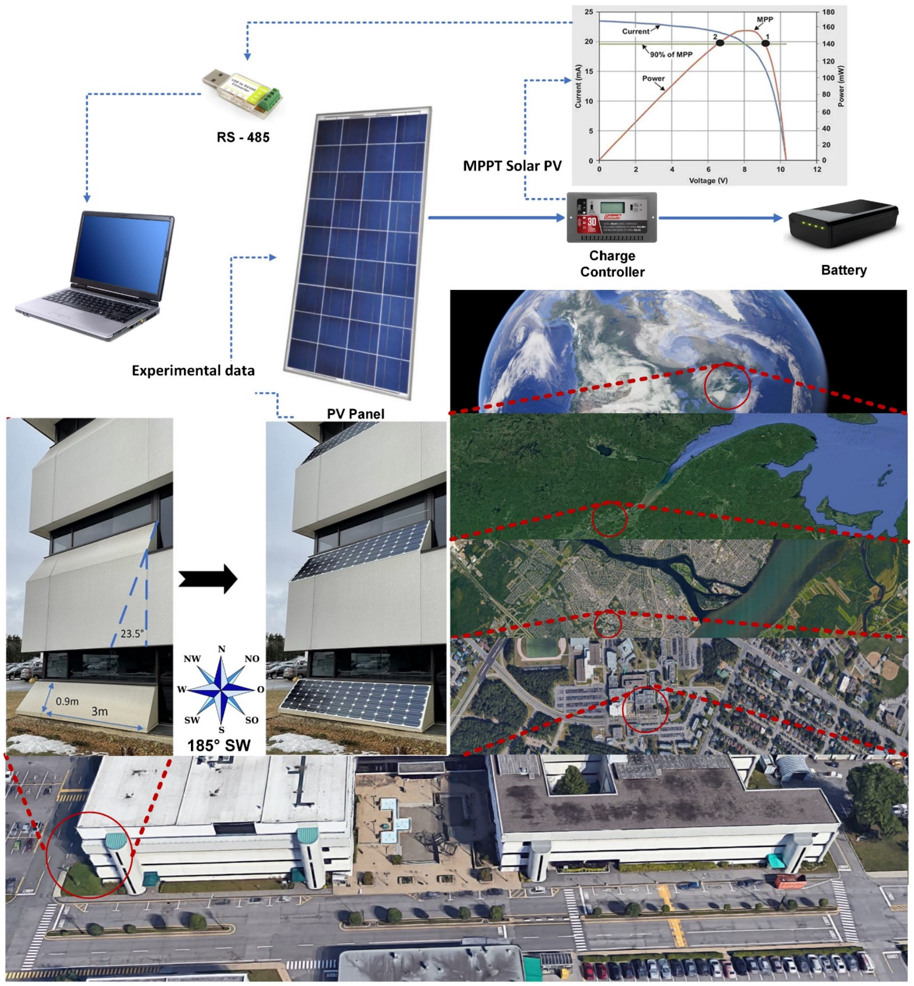

Figure 8 The PV location, direction and position

A promising method for estimating future available energy employs ML techniques to discern available energy for specific times or extended durations. An accurate and reliable ANN model is essential for predicting the available energy from PV panels. To realize this, input parameters must be judiciously chosen based on their marked impact on PV panel output. As indicated by Eq. (1), temperature, visibility, humidity, air pressure, wind speed, and hourly solar irradiation are chosen as input parameters, illustrated in Figure 9, due to their strong correlation with the performance of PV panels. Furthermore, factors like azimuth and tilt angle, capacity factor, efficiency, cover ratio, system losses (including mismatch, wiring, and connections), power control, ageing, and light-induced degradation will be inherently incorporated into the outcome when training the ANN with experimental data. To guarantee model precision, genuine data gathered from a solar panel over a year was employed for both training and validation. A feed-forward neural network was adopted to forecast future electricity production from a PV system based on historical data. This neural network was preferred because of its proficiency in accurately depicting intricate nonlinear associations between input and output data, making it ideal for solar energy production prediction. The dataset was divided into training, validation, and test sets using a 76/12/12 ratio. The training set enabled the NN's education, the validation set fine-tuned the NN hyperparameters and curbed overfitting, while the test set gauged the performance of the finalized model. Data processing comprised feature selection, normalization, and standardization, which bolstered the NN model's precision. Furthermore, early stopping during training and regularization approaches like L1 and L2 regularization, which penalize hefty weights, helped mitigate overfitting. In sum, based on its adeptness in precisely modeling complex nonlinear relations and the training, validation, and testing methodologies adopted, the feed-forward neural network emerged as the most fitting NN for this undertaking.

Figure 9 illustrates that this ANN has six inputs, two hidden layers, and one output layer. Pertaining to the model's design, a neural network structure featuring two hidden layers was chosen, grounded on past studies vouching for its efficacy in accurately forecasting PV panel output [89]. Deciding on the number of hidden layers in an ANN is pivotal for attaining supreme prediction accuracy. Generally, two hidden layers are employed as they have proven to strike an equilibrium between overfitting and underfitting. Moreover, the neuron count per layer ought to be carefully determined based on the problem's intricacy and the dataset's volume. Upon evaluating diverse algorithms, the Conjugate Gradient with Powell-Beale Restarts emerged as the most adept for training this predictive PV production model. It was chosen since it converges more swiftly and yields more precise outcomes compared to other optimization algorithms. The conjugate gradient method occasionally readjusts its search direction to the negative gradient. Ultimately, a standard reset point is achieved when the iteration count matches the network parameters [90]. As tested with Eq.(2), where 'g' symbolizes the gradient, meeting this condition signifies that the search direction will revert to its negative counterpart.

$$|g_{k-1}^T g_k| \geq 0.2 g_k^2 \tag{2}$$

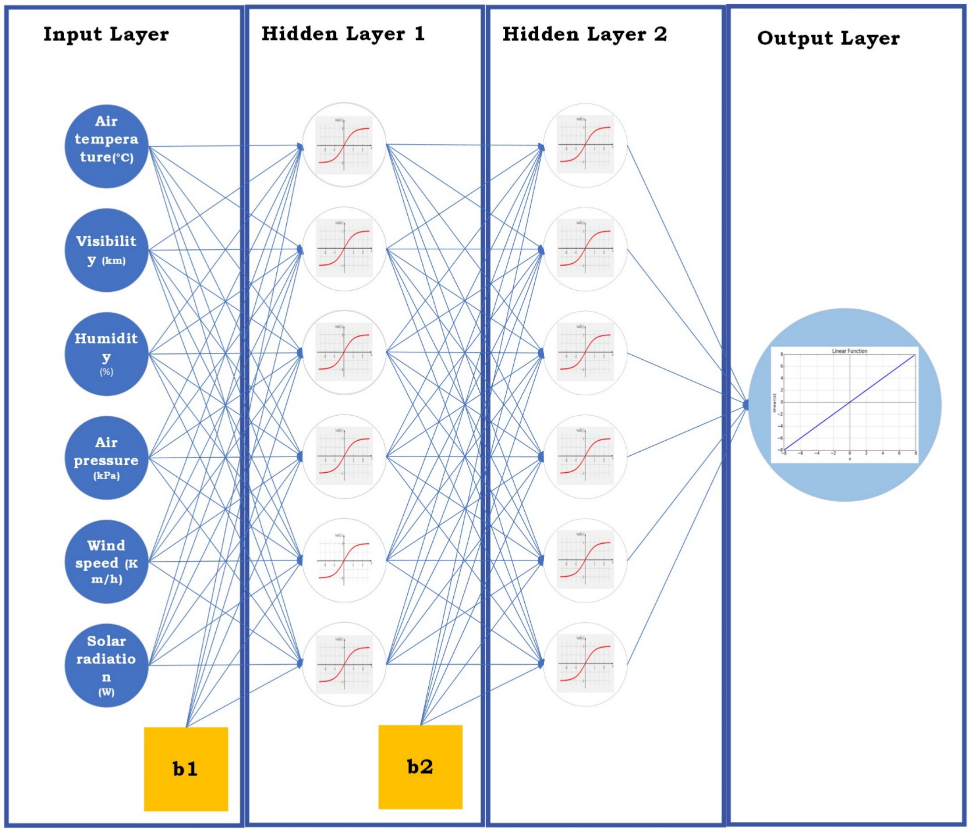

Figure 9 The ANN design for the predictive PV production model

In summary, the chosen input parameters, data preprocessing methods, and the neural network architecture combined with its algorithm are anticipated to offer a strong and efficient solution for forecasting the potential available energy of PV panels. This approach also aims to sidestep overfitting while maintaining high prediction accuracy.

Eq.(3) assists in estimation and scaling in relation to Eq.(7) through Eq.(10). Upon examining models related to PV output DC power, both Eq.(3) and Eq.(4) underscore that maintaining the PV at its optimal efficiency point significantly influences the energy harvested.

$$n_p . P_{pv} . \eta_{array} \approx n_{el} . P_{el} \tag{3}$$

In these equations, n_p and n_{el} denote the number of panels and electrolyzers, respectively, while P_{pv} and P_{el} represent the output power of a PV panel and the required power for PEMWE, respectively. Additionally, the overall efficiency of the PV array (η_{array}) should be taken into account.

$$\alpha\mathrm{HyPro}_S = \alpha PV_{max} \times \alpha\mathrm{PEM} \times \mathrm{CP}_{PV} \tag{4}$$

$$\mathrm{CP}_{PV} = (\mathrm{Output}_{\mathrm{PV}}/\mathrm{Output}_{\mathrm{max}}) \tag{5}$$

According to Eq. (4), enhancing the efficiency of both the PV and PEMWE will elevate the overall efficiency of HyPro. However, there is a coefficient that is contingent upon the structure and design. By refining the design of a PEMWE, an increase in HyPro efficiency is projected. In Eq. (4),

$\alpha HyPro_S$ represents the efficiency of the HyPro system within a stack. This efficiency is influenced by the combined efficiencies of the PV and PEMWE, and it incorporates a coefficient of performance (CP_{PV}). Thus, an optimal design enhances the performance of auxiliary systems, facilitating synergy between electrolysis and PV, and ultimately boosting the efficiency of the entire system.

3.2. Hydrogen Production

The energy pattern identified in the previous section should be employed to evaluate an electrolysis system for HyPro utilizing solar energy. To compute the HyPro, a PEMWE model is developed based on experimental data gathered from a setup depicted in Figure 10. The specifications of this electrolyzer, along with its environmental attributes, are detailed in Table 3. As seen in Figure 10, one side of the PEMWE is connected to the deionized water supply, while the other is linked to a power supply. An Ethernet network enables a computer to monitor and regulate a programmable power source. Moreover, the electrolyzer's output is attached to a flowmeter before it feeds into the H2 tank, where a data logger captures its real-time information. Consequently, by controlling and recording the input electricity and the output H2, and by monitoring the cell data, the performance of the electrolyzer models can be comparatively assessed.

Table 3 Working and environmental characteristics of the PEMWE

Lab. Location		**Institut of Hydrogen Research (IHR) Trois-Rivieres, QC, Canada**	
Lab. Average temperature		24.4 °C	
Water Average temperature		24.2° W	
Electrolyzer Type		PEMWE	
PEMWE Manufacturer		Shandong Saikesaisi Hydrogen Energy [91]	
model		QLC-1000	
Number of cells		4	
Input voltage		12 V	
Input current		36 A	
Max. voltage		15 V	
Max. current		40 A	
H2 Production		1 L /min	
O2 Production		500ml/min	
Operating temperature		5-45 °C	
Output-pressure		0-145 psi	
Stack Diameter		13.8 cm	
Power supply (DC)		100 Volt * 100 Amper (Programmable)	
FLOW METER		**Storage Tank**	
Flow range	10 L/min	Capacity	10 L
Accuracy	±1%	Material	steel
Maximum Gas Pressure	250 psig	Max. Working Pressure	200 psi

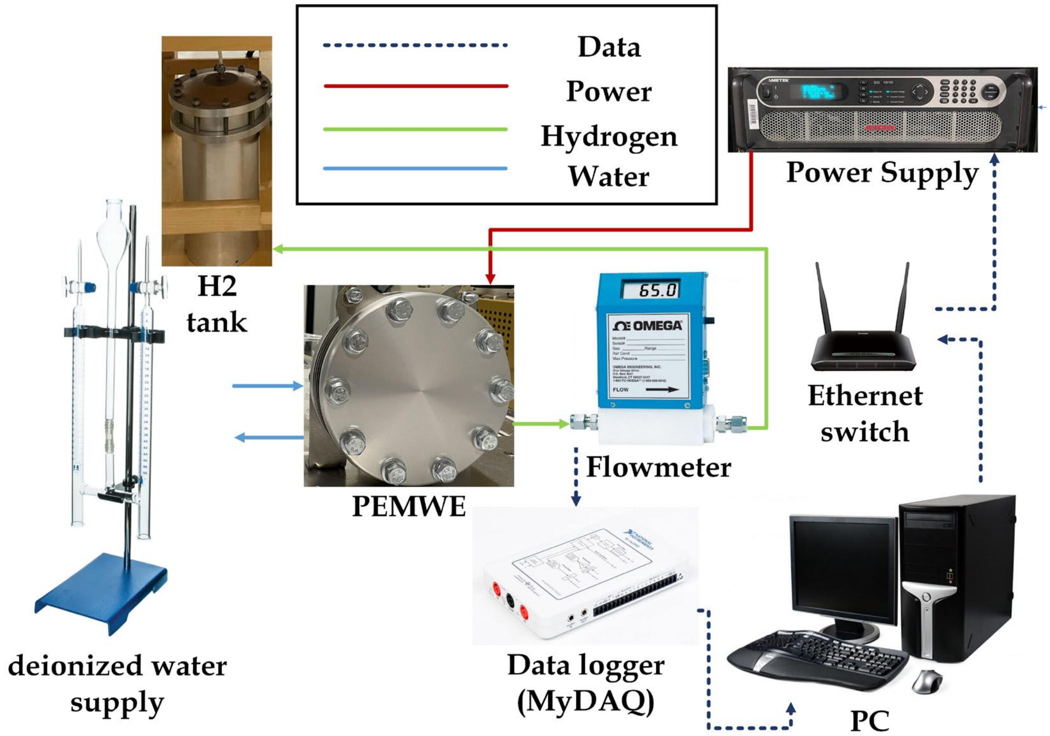

Figure 10 PEMWE, auxiliary and connections testbench

3.2.1. Basics

HyPro occurs within the cells of the PEMWE. This process not only offers an efficient and clean method of producing H2 from water, but it also yields O_2 as a byproduct. In a stack section, a zero-gap cell fitted with a solid polymer electrolyte facilitates proton conduction, separates the produced gases, and electrically insulates the electrodes. H_2 and O_2 are produced through reactions in the cathode (Eq.(7)) and anode (Eq.(6)) sides, as well as the catalyst layers. The role of electricity in this process is evident in Eq.(8).

$$H_2O = \left(\frac{1}{2}\right) O_2 + 2H^+ + 2e^- \tag{6}$$

$$2H^+ + 2e^- = H_2 \tag{7}$$

$$\mathrm{H_2O} + \text{ electricity} = \mathrm{H_2} + \left(\frac{1}{2}\right) \mathrm{O_2} \tag{8}$$

The voltage and current of this electricity are influenced by various parameters. If the process takes place under reversible conditions, implying that no exergy or enthalpy is consumed and no losses occur, then the potential difference at the electrodes would be 1.229 V. This is referred to as the reversible cell voltage (V_{rev}^0). Without an external heat source, the total energy required for the reaction (ΔH_R^0) must come from electrical energy. However, when the necessary thermal energy contribution is available, only minimal electrical work is needed to split the water. As a result, the required voltage exceeds V_{rev}^0 and is termed the thermoneutral voltage V_{th}^0 in its standard state, as described in Eq.(9). Additionally, the Higher Heating Value of Hydrogen (HHVH) remains constant, approximately 3.54 kWh/Nm^3 [92-94].

$$V_{th}^{0} = \frac{\Delta H_R^0}{z.F} = 1.481\,V \tag{9}$$

Where z represents the number of moles of electrons transferred in the reaction and F denotes the Faraday constant, with a value of $9.6485 \times 10^4\ C/mol$. For an accurate estimate, the precise cell voltage (V_{cell}) is necessary. This voltage is determined by dividing the thermoneutral voltage by the cell efficiency (η_c), , as indicated in Eq.(10). The electrical work can be derived from Eq.(11), where η_f represents the faradic efficiency. This value approximates 285.8 J/mol or 0.08 Wh/g..

$$V_{cell} = \frac{V_{th}^0}{\eta_c} \tag{10}$$

$$W = zF\frac{V}{\eta_f} \tag{11}$$

3.2.2. Performance and efficiency of PEMWE in experimental tests

Generally, the performance of the electrolyzer is represented through the use of polarization curves. Polarization curves provide valuable insights into the performance of the electrolysis system under various operating conditions. They illustrate the relationship between cell potential and current density, aiding in the identification of optimal operating conditions. In this study, experimental data from the PEMWE (Proton Exchange Membrane Water Electrolysis) were collected to generate efficiency and polarization curves.

As shown in Figure 11, the voltage and efficiency of the PEMWE stack are illustrated based on the current. The blue axis (left side) represents efficiency as a percentage, while the red axis (right side) indicates the voltage level. These curves were plotted using experimental data, which have been deemed a reasonable and reliable approximation for the behavior of the electrolyzer.

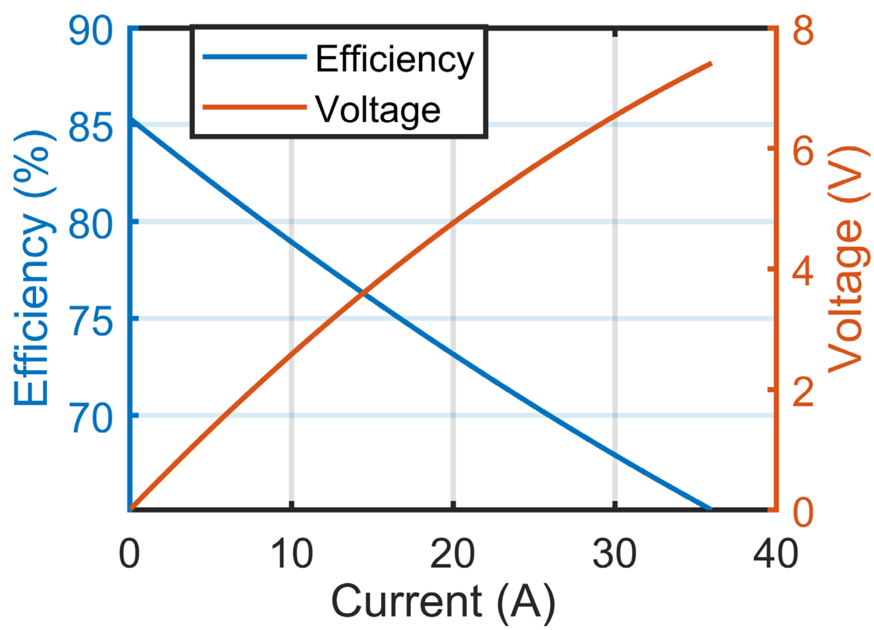

Figure 11 PEMWE polarization and efficiency curves

Observations from the literature indicate that the actual cell voltage (V_C) of a PEMWE, as measured experimentally in this specific case, is the cumulative result of its reversible (open circuit) voltage (V_o) and various overvoltages [95]. These overvoltages, termed activation (U_{ac}), ohmic (U_{oh}), and concentration (U_{co}) as per Eq.(13), significantly influence the polarization curve of the PEMWE. Each of these overvoltages impacts different segments of the polarization curve. However, it is important to note that, in this instance, the concentration overvoltage has not been factored into the calculation and scaling, including its corresponding area.

$$P_c = I_C \times V_C \tag{12}$$

$$V_C = V_o + U_{ac} + U_{oh} + U_{co} \tag{13}$$

Equation (12) is formulated for an individual cell; however, the current and voltage of a stack depend on the configuration of the system. Equation (14) illustrates the relationships for stack current (I_S) and voltage (V_S). In the case of an array connected in series, as shown in Equation (15), the voltage at the terminals of the stack is the accumulation of voltages across the series connections (with each cell's current being I_{cn}). Conversely, when the array is connected in parallel, as demonstrated in Equation (16), the stack current equals the sum of currents flowing through the parallel-connected cells (with each cell's voltage being V_{cn}) [96].

$$P_s = I_s \times V_s \tag{14}$$

$$P_s = I_s \times \sum_{n=1}^{N} V_{cn} \tag{15}$$

$$P_s = V_s \times \sum_{n=1}^{N} I_{cn} \tag{16}$$

Utilizing these relationships, the variable quantity of HyPro can be described using Equation (17). Within this equation, 'N' represents the number of cells, while 'η_e' signifies the dynamic amount of PEMWE efficiency as determined by Equation (18), and this efficiency is linked to the current.

$$\int_0^t f_{H2}.\,dt = \frac{\int_0^t N \times I \times V \times \eta_e \times dt}{HHVH} \tag{17}$$

$$\eta_e = 0.00293I^2 - 0.667I + 85.333 \tag{18}$$

To estimate the efficiency of the electrolyzer (η_e) using Equation (18), based on the current from the solar panel, a second-order polynomial equation is employed from Figure 11. The equation is interpolated using experimental data and applied through approximation in this context.

Building upon the experimental outcomes of a small-scale electrolyzer, the behavior of an electrolyzer with a different number of cells can be predicted by maintaining the actual cell ratio.

Various scaling formulas can be utilized to extrapolate the behavior of large-scale electrolyzers from the experimental findings of smaller-scale counterparts. Equation (19) offers a summarized illustration of size conversion within the calculations. When upscaling the production of a small electrolyzer, determining the suitable size for a larger system can be facilitated by calculating the required increase in the number of cells. However, it is crucial to highlight that scaling laws may not consistently yield accurate results due to variations in operating conditions, materials, and other contributing factors. Experimental validation is necessary for confirming the outcomes of scaled-up systems [97, 98].

$$V_S = N(V_o + U_{ac} + U_{oh}) \tag{19}$$

The energy efficiency coefficient of an electrolysis system quantifies the effectiveness of converting electrical energy into H_2 and O_2 gases through water electrolysis, as depicted in Equation (20). It is formulated as the ratio of the energy content of the produced H_2 and O_2 gases (W_{rev}) resulting from electrolysis to the overall energy input into the system (W_{irrev}), encompassing all associated losses (such as energy and current losses, heat dissipation, etc.) occurring within the electrolysis unit cell/stack and supplementary subsystems (e.g., heat exchangers, pumps, etc.).

In practical and industrial contexts, this definition is commonly employed. Conversely, in academic and scientific research, the focus often centers on the water electrolysis reaction exclusively, within the confines of constant temperature and pressure conditions. The energy efficiency coefficient of an electrolysis system takes into consideration all parasitic losses, amalgamating them as the denominator of the equation. The numerator comprises the energy content of H2/O2 gases produced by electrolysis. This coefficient is determined as the ratio of the energy content of the products obtained at the exhaust of the system to the overall energy supplied [99].

$$\varepsilon_{PEMWE} = \frac{W_{rev}}{W_{irrev}} \tag{20}$$

3.2.3. Degradation

PEMWE degradation can be characterized by voltage decay over time under constant operating conditions. The simplest model to describe this behavior is based on empirical observation. This assumes that the voltage loss is proportional to the logarithm of the operating time [100]:

$$V_t = V_0 - d\ln(t/t_r) \tag{21}$$

Here, V_0 represents the initial voltage, 't' stands for the operating time, t_r is a reference time, and ' d ' represents the degradation rate constant. According to Voronova et al.'s research [101], under solar fluctuating conditions, this degradation rate can be approximated as 3.5 mV/h. Various degradation mechanisms are accounted for in more intricate models, encompassing catalyst degradation, membrane degradation, and issues related to water management. Typically, these models entail a higher number of parameters, necessitating a more comprehensive dataset from the experimental phase to accurately calibrate the model's parameters. [102, 103].

3.3.Modular PEMWE

As elucidated in Section 2, the utilization of modular systems plays a highly effective role in both controlling and enhancing the operational conditions and efficiency of the HyPro system. Their inherent structure not only facilitates system capacity expansion, but also significantly simplifies energy management and control, resulting in heightened efficiency. Furthermore, the integration of diverse and capable auxiliary systems is viable, as detailed in Section 2.3.

In this work, the structure employed for the proposed modular PEMWE system is depicted in Figure 12. Since the intended placement is within a university building, specific limitations and opportunities have arisen. Although space is confined, the availability of internal building facilities and water access remains convenient. Given that the primary focus of our project centers around comparing single-stack and modular PEMWE systems in terms of HyPro, other parameters such as cost and size are not extensively discussed in this study. The architectural layout is divided into two accessible buildings, accommodating two water reservoirs and H_2 tanks to enhance safety and compactness.

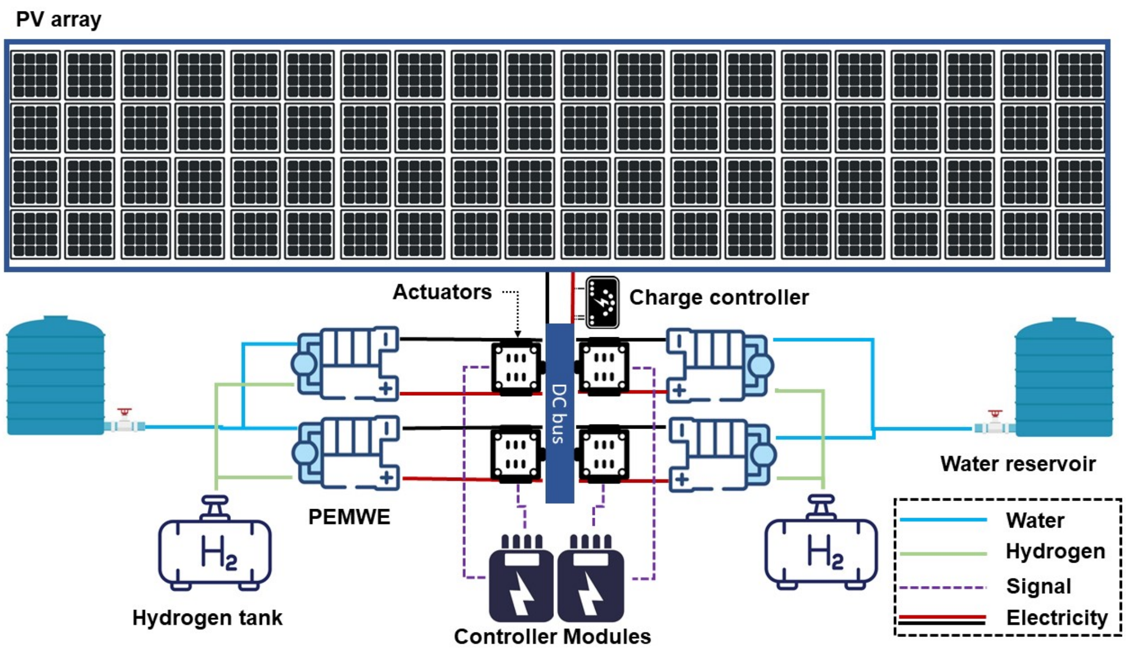

Figure 12 Proposed structure for modular PV and electrolyzer

In the ANN model, the proposed array can generate a maximum energy output of around 10 kW. To compare the HyPro system using both a modular PEMWE setup and a single-stack configuration, we investigate two cases in this study.

In the first case, a single-stack 10 kW electrolyzer with 80 cells is used for the HyPro application. In the second case, four medium-sized electrolyzers with a maximum input power of 2.5 kW and 20 cells each are employed. The generated energy is then transferred to a DC bus through a charge controller designed to maximize solar energy utilization, as depicted in Figure 8. Subsequently, the controller modules determine the distribution of electrical current among the PEMWEs. The power-sharing strategy implemented follows the principles outlined by Guilbert and Vitale [67].

Table 4 presents four distinct scenarios that cover the range from zero to the maximum available energy from the PV array. In scenario 1, if the available energy is less than 2.5 kilowatts, only one PEMWE will be responsible for HyPro. In scenario 2, when the available power falls between 2.5

and 5 kW, two of the PEMWEs will be activated. For scenario 3, if the total power output surpasses 5 kW but remains below 7.5 kW, three PEMWEs will be operational. Finally, in scenario 4, if the available energy exceeds 7.5 kW/h, all of the electrolyzers will be engaged for HyPro.

Table 4 Power allocation strategy based on available energy

Scenario	P	PEMWE 1	PEMWE 2	PEMWE 3	PEMWE 4
1	2.5 kW > P	On	Off	Off	Off
2	5 kW > P > 2.5 kW	On	On	Off	Off
3	7.5 kW > P > 5 kW	On	On	On	Off
4	P > 7.5 kW	On	On	On	On

4. Results and discussion

In the preceding section, the process of predicting the HyPro amount was outlined. This involved initially deriving the available energy quantity through a precise model reliant on environmental conditions, coupled with experimentation on a control sample panel, as discussed in Section 3.1. Subsequently, an evaluation of the actual HyPro amount derived from solar energy was conducted, as detailed in Section 3.2. As the concluding step, the HyPro values for the theoretical project were juxtaposed for both the proposed single PEMWE configuration and the modular PEMWE setup, elucidated in Section 3.3.

4.1.Available energy by ANN model

The assessment of the ANN's performance encompassed three distinct stages: training, testing, and validation, as illustrated in Figure 13. The training phase involved fine-tuning the ANN's parameters using a subset of the available data. In the subsequent testing phase, the model's capacity for generalization was appraised by applying it to a distinct dataset. The validation phase, on the other hand, gauged the model's efficacy in handling newly acquired and previously unseen data.

The performance of the ANN model was remarkably robust, exhibiting accuracy across all phases. Specifically, the performance metrics were calculated as 0.9994 for the training phase, 0.99941 for the testing phase, and 0.99944 for the validation phase. These results strongly indicate the ANN's ability to effectively learn from the input data and generalize its insights to various contexts.

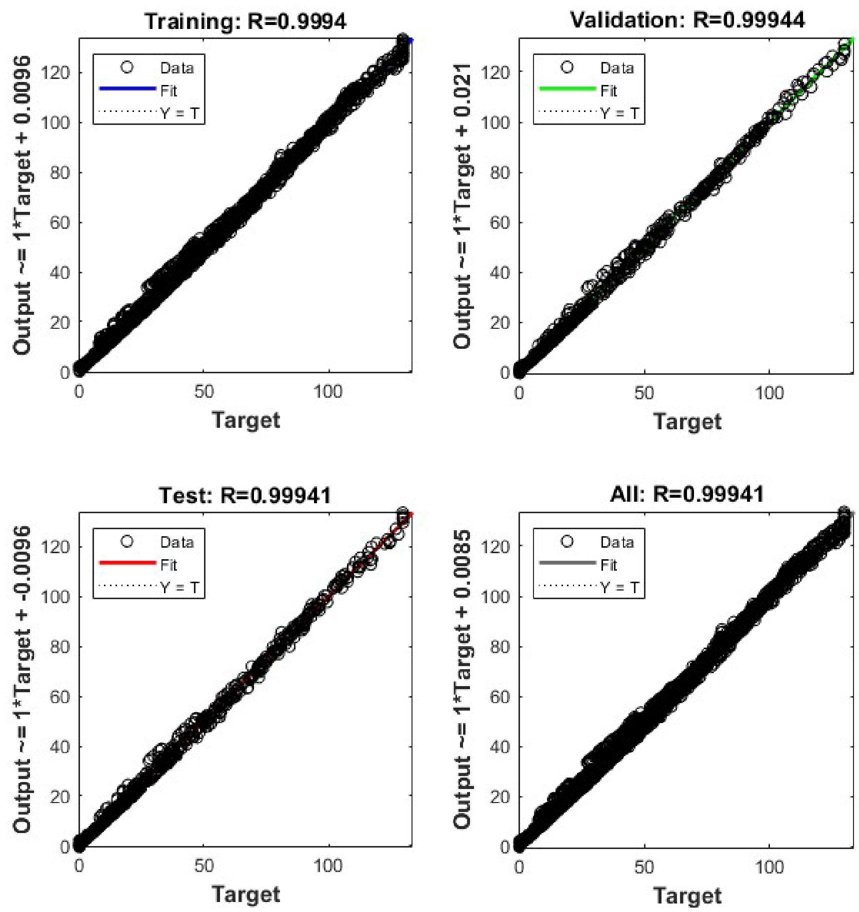

Figure 13 PEMWE ANN model regression

The trained ANN effectively demonstrated its capability to predict solar energy levels in Trois-Rivières, grounded in the chosen input variables and reference data. The features selected, encompassing aspects such as sun irradiation quality and the influence of temperature on photovoltaic (PV) efficiency, proved pivotal in accurately forecasting available energy. Rigorous validation against experimental data confirmed the reliability of the ANN model, yielding outcomes that closely aligned with actual measurements, differing by a mere 6.3%.

These findings underscore the ANN model's potency as a robust tool for solar energy prediction, offering substantial implications for the strategic planning and operational efficiency of PV systems. On the whole, these results exemplify the potential harnessed by machine learning methodologies within the realm of renewable energy. Additionally, they underscore the critical role played by judicious selection of input variables and meticulous calibration of model parameters, both instrumental in attaining precision in predictions.

4.2. Hydrogen Production using a single-stack system

In this section, we present the daily HyPro amount based on observations derived from laboratory tests. Figure 14 illustrates solar radiation levels in Trois-Rivières, along with the energy harvested and the resulting H2 production. This dataset stems from a sunny day's (approximately 15 hours) experimentation conducted in July 2022. For this test, the energy generated by two panels, as detailed in Table 2, powered a 1000 ml per hour electrolyzer. Notably, the HyPro algorithm closely mirrors the anticipated solar energy production pattern. Consequently, the HyPro output for this specific test day and power supply configuration reached a cumulative total of around 4.27 liters.

It is imperative to factor in the disparities in performance and efficiency between a singular PEMWE stack and an upscaled version when evaluating the overall electrolyzer performance. Precise utilization of scaling factor coefficients assumes paramount importance to ensure exact calculations. Moreover, incorporating experimental data from an electrolyzer possessing the same dimensions as the scaled-up stack would undoubtedly enhance the result accuracy.

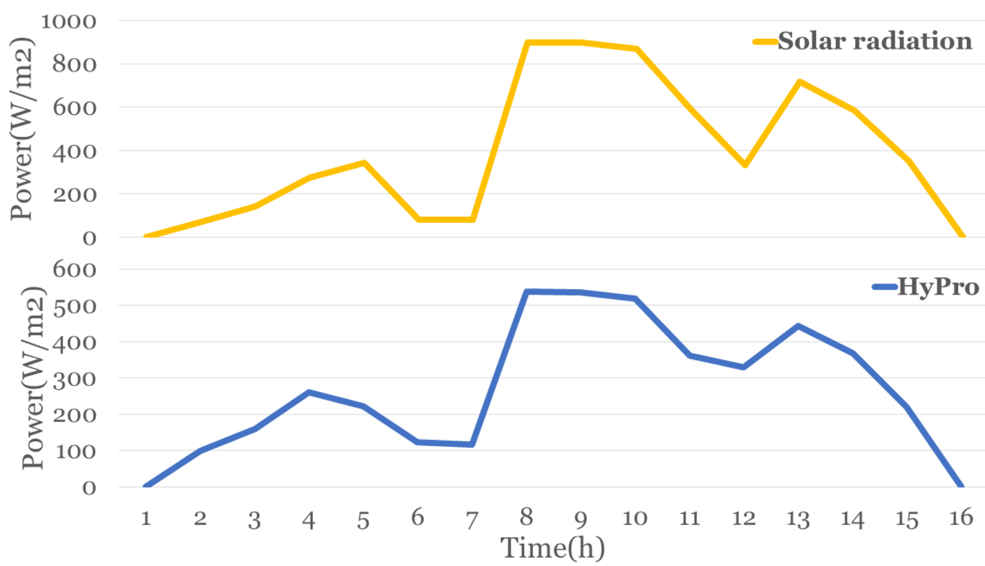

Figure 14 HyPro with a single-stack PEMWE supplied by PV in a day

4.3. Hydrogen Production using a modular structure

As described by Equation (18), the efficiency of the PEMWE is variable, contingent on the current density. This dynamic characteristic can be adeptly managed and optimized by judiciously distributing input power within a modular framework. To achieve this, a power allocation strategy is employed to ensure a consistent power supply to the PEMWE, thereby maintaining efficiency at its peak potential, as indicated in Table 4. This approach yields two key advantages: firstly, by turning off specific PEMWE stacks, system degradation is mitigated; secondly, HyPro benefits from leveraging the complete range of optimized stacks. This intricate interplay is illustrated in Figure 11, where the relationship between current density and PEMWE efficiency is depicted. Observing the PEMWE polarization and efficiency curves presented in Figure 11, it is discernible that PEMWE efficiency can exceed 70% when current remains below 27 A. Notably, in three of the scenarios, at least one PEMWE is inactive, thereby preserving its integrity and decreasing overall system degradation.

With this insight, HyPro estimation in Trois-Rivières is undertaken for a year, comparing the outcomes with a single-stack PEMWE operating at high capacity and direct current from the PV array, against a modular structure employing a control strategy for maintaining constant current to the PEMWE. Figure 15 vividly showcases the substantial impact of implementing a modular structure with controlled current allocation on HyPro. This approach is projected to yield remarkable improvements in HyPro throughout the year, with a pronounced effect during the elongated days of summer. AI-assisted estimates suggest that PV panel installation, coupled with solar energy conversion to H2, can yield over 2716 liters of H2 annually. However, when factoring in the modular structure and energy control strategy, this figure escalates by 33.36% to reach 3622 liters annually. Moreover, the modular structure not only curtails system degradation but also enhances capacity by boosting overall system efficiency, leading to an additional production of approximately 906 liters compared to conventional methods.

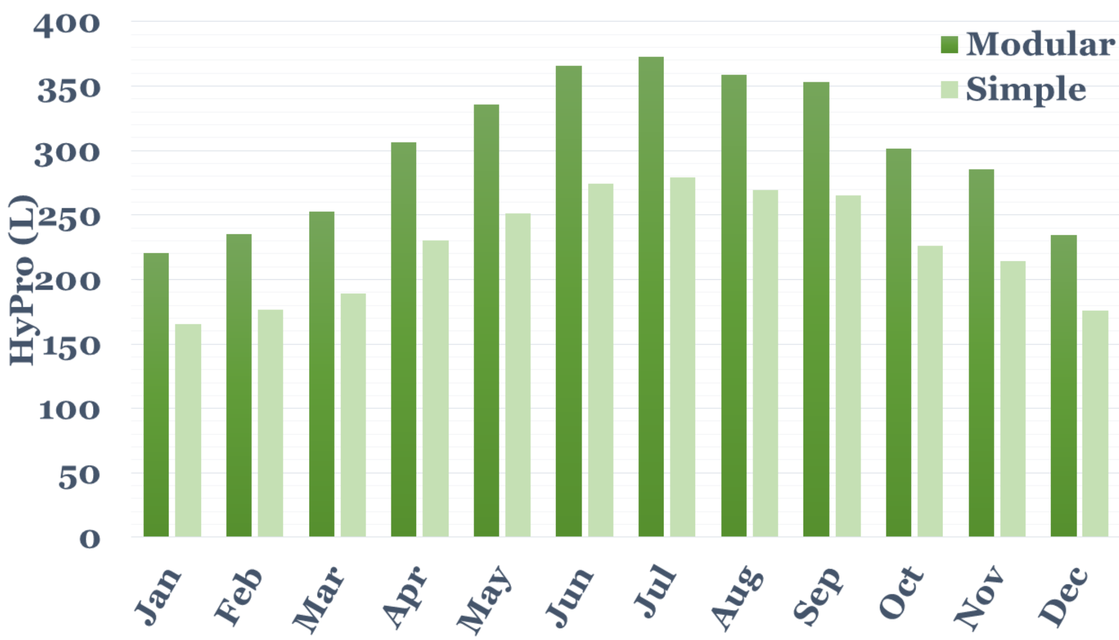

Figure 15 Comparision of HyPro with a modular and simple system

Figure 16 presents the available solar energy for the proposed PV array on a sunny summer day, elucidating the contrasting impacts of the modular system and the single-stack HyPro configuration. The modular power allocation scheme is adept at optimizing solar energy utilization. Notably, the green electrolyzer icon signifies the PEMWEs that are operating at efficiency levels exceeding 70%, consistently maintained in the modular structure, whereas this uniformity isn't realized in the case of a single PEMWE.

Furthermore, Figure 16 also visualizes the degradation rates. Intriguingly, the likelihood of degradation for PEMWEs one through four stands at 1, 0.75, 0.5, and 0.25, respectively. This finding is noteworthy due to the inherent ease of replacing electrolyzers within modular systems.

The graphical representation in Figure 16 effectively underscores the advantages conferred by the modular setup, particularly in terms of efficiency maintenance and degradation management, both of which contribute significantly to enhanced system performance.

The computation of total efficiency, as expressed in Equation (17), incorporates the consideration of both the scaled-up coefficient and the efficiency associated with scaling up the system. Scaling up a PEMWE encompasses several intricate adjustments, including augmenting the active surface area of the electrodes, calibrating catalyst loading, modulating electrolyte and cooling water flow rates, and potentially adapting the membrane thickness to maintain the overall current density of the electrolyzer.

Moreover, in the process of enlarging the PEMWE system, the escalated power requirements must be taken into account, given that they may increase proportionately with the system's dimensions. In essence, optimizing the scale-up of a PEMWE necessitates a meticulous examination of multiple factors, requiring a comprehensive approach to ensure consistent or even enhanced system performance. The successful execution of this scale-up strategy hinges on a thorough understanding of these considerations and their seamless integration into the design and operation of the larger system.

Figure 16 Comparing the performance of using modular and conventional systems for HyPro from solar energy graph

Comparing the voltage degradation of a single PEMWE stack and a modular PEMWE system over a span of 7000 hours offers valuable insights into the relative robustness of these configurations. The collected data reveals that the single PEMWE stack exhibited a higher voltage degradation rate, with a reduction of 37.4 V over the 7000-hour period, equating to a degradation of 15.58%. In stark contrast, the modular PEMWE system displayed notably lower voltage degradation rates. Specifically, PEMWE 1 experienced a 5.9 V reduction, PEMWE 2 saw a 5.3 V decrease, PEMWE 3 registered a 4.1 V decrease, and PEMWE 4 exhibited a mere 3.8 V reduction. These degradation rates translate to 10%, 8.8%, 6.8%, and 6.3%, respectively. Remarkably, the average degradation across the modular system is approximately 7.6% lower than that of the single-stack setup.

This data underscores the potential of the modular PEMWE system to exhibit greater durability and resistance to voltage degradation in comparison to the traditional single-stack arrangement. Thus, the adoption of a modular structure coupled with strategic power allocation emerges as a compelling approach to elevate HyPro, extend the lifespan of PEMWEs, and mitigate degradation. It is imperative to note, however, that further exploration is warranted to pinpoint the root causes of degradation and validate the accuracy of the estimated outcomes. Additionally, it is crucial to acknowledge that the rate of degradation is influenced by an array of factors, encompassing operating conditions, design parameters, and the materials employed. Consequently, meticulous consideration and optimization of these variables hold paramount importance in enhancing the overall durability and performance of the PEMWE system.

5. Conclusions

Renewable energies are becoming increasingly appealing in conjunction with PEMWEs due to their capacity to store energy as environmentally friendly, efficient, and potent hydrogen (H2). However, a significant challenge associated with Renewable Energy Sources (RES) is their inherent intermittency, which can substantially impact the performance and efficiency of PEMWE systems. This intermittency not only undermines the efficiency of the PEMWE system but also accelerates its degradation and diminishes its operational lifespan. Consequently, optimizing the power supply to PEMWEs becomes paramount in mitigating degradation and enhancing the overall energy efficiency of the system.

The present study employs a machine learning-based approach to predict HyPro via solar energy in the city of Trois-Rivières. It further compares the outcomes of a conventional PEMWE system with those of a modular design. The predictive model, trained using experimental data collected from PV panels and neural networks, investigates the viability of converting solar energy into H2 through a PEMWE model validated by experimentation. A comparison between the HyPro outputs in normal and modular modes is conducted by regulating input energy. Control over the PEMWE system's input current is attained through a power allocation mechanism.

The results obtained underscore the significant benefits of a modular structure for HyPro, manifesting in an approximate 33% surge in HyPro. Moreover, the proposed modular configuration holds the potential to curtail electrolyzer degradation by around 7.6%, ultimately extending its operational lifespan.

Further research endeavors are imperative to enhance PEMWE efficiency through RES and to delve deeper into optimizing arrangements for green HyPro. Additionally, it is vital to account for PEMWE efficiency across various scales and systems, given its susceptibility to variations under diverse operating conditions.

Nomenclature:

A_L	**Active large surface area (mm)**
A_S	Active small surface area (mm)
B_r	temperature coefficient
CP_{PV}	Coefficient of Performance
G_{nr}	Solar irradiance (W/m^2)
I_C	cell current (A)
I_S	stack current (A)
I_{cn}	each cell current (A)
P_C	cell power (W)
P_{el}	electrolyzer required power
P_{pv}	PV Power (W)
T_{pv}	PV temperature(°C)
T_r	operating reference temperature (°C)
U_{ac}	Activation overvoltage (v)
U_{co}	Concentration overvoltage (v)
U_{oh}	Ohmic overvoltage (v)
V_C	cell voltage (v)
V_O	reversible (open circuit) voltage (v)
V_S	stack voltage (v)
V_{cell}	cell voltage (v)
V_{cn}	each cell voltage (v)
V_{rev}^0	reversible cell voltage (v)
V_{th}^0	thermoneutral voltage (v)
n_{el}	number of electrolyzers
n_p	number of PV panels
t_r	reference time
$\alpha HyPro_S$	HyPro system (in a stack) efficiency
α_{PV}	PV cell efficiency (%)
η_{array}	PV array efficiency
η_c	cell efficiency (%)
η_e	Electrolyzer efficiency (%)
A	Area (square meter, m^2)
E	Energy ($Wh \approx 3600\ joules$)
f	gas flow rate (Normal Meter Cubed per Hour Nm3/hr)
F	Faraday constant (C/mol)
g	gradient
$HHVH$	Higher Heating Value of Hydrogen (kWh/Nm^3)
P	Power (W)
Rct	charge transfer impedance (Ohm)
t	Time (h and H/2)
W	electrical work of electrolysis (J/mol)
W_{irrev}	Irreversible energy (J/mol)
W_{rev}	Reversible energy (J/mol)
Υ	surface coverage ratio (/)
ΔH_R^0	Electrolysis required energy (J/mol)

Abbreviations:

AC	**Alternating Current**
ANN	Artificial Neural Network
CNC	Computer Numerical Control
CO_2	Carbon Dioxide
DC	Direct Current
e^-	electron
ERC	Ejector Refrigeration Cycle
FC	Fuel Cell
H_2	Hydrogen
HyPro	Hydrogen Production
kW	Kilo Watt
L	Liter
MES	Modular energy system
ML	Machine Learning
MW	MegaWatt
NPV	Net present value
O_2	Oxygen
ORC	Organic Rankine Cycle
PEMFC	Proton Exchange Membrane Fuel Cell
PEMWE	Proton Exchange Membrane Water Electrolyzer
PTC	Parabolic Trough (solar) Collector
PtG	Power-to-Gas
PV	Photovoltaic
RES	Renewable Energy Source
RO	reverse osmosis
WECS	wind Energy Conversion System

Acknowledgements

This work was supported in part by the Natural Sciences and Engineering Research Council of Canada (NSERC) (2018-06527)

References

[1] M. Younas, S. Shafique, A. Hafeez, F. Javed, and F. Rehman, "An Overview of Hydrogen Production: Current Status, Potential, and Challenges," *Fuel,* vol. 316, p. 123317, 2022/05/15/ 2022, doi: https://doi.org/10.1016/j.fuel.2022.123317.

[2] D. Wu, D. Wang, T. Ramachandran, and J. Holladay, "A techno-economic assessment framework for hydrogen energy storage toward multiple energy delivery pathways and

grid services," *Energy,* vol. 249, p. 123638, 2022/06/15/ 2022, doi: https://doi.org/10.1016/j.energy.2022.123638.

[3] Q. Hassan *et al.*, "Renewable energy-to-green hydrogen: A review of main resources routes, processes and evaluation," *International Journal of Hydrogen Energy,* 2023/02/10/ 2023, doi: https://doi.org/10.1016/j.ijhydene.2023.01.175.

[4] A. Makhsoos, M. Kandidayeni, B. G. Pollet, and L. Boulon, "A perspective on increasing the efficiency of proton exchange membrane water electrolyzers– a review," *International Journal of Hydrogen Energy,* 2023/01/27/ 2023, doi: https://doi.org/10.1016/j.ijhydene.2023.01.048.

[5] Á. Hernández-Gómez, V. Ramirez, D. Guilbert, and B. Saldivar, "Development of an adaptive static-dynamic electrical model based on input electrical energy for PEM water electrolysis," *International Journal of Hydrogen Energy,* vol. 45, no. 38, pp. 18817-18830, 2020/07/31/ 2020, doi: https://doi.org/10.1016/j.ijhydene.2020.04.182.

[6] F. Barbir, "PEM electrolysis for production of hydrogen from renewable energy sources," *Solar Energy,* vol. 78, no. 5, pp. 661-669, 2005/05/01/ 2005, doi: https://doi.org/10.1016/j.solener.2004.09.003.

[7] S. Rahimi, M. Meratizaman, S. Monadizadeh, and M. Amidpour, "Techno-economic analysis of wind turbine–PEM (polymer electrolyte membrane) fuel cell hybrid system in standalone area," *Energy,* vol. 67, pp. 381-396, 2014/04/01/ 2014, doi: https://doi.org/10.1016/j.energy.2014.01.072.

[8] S. A. Communications. "Siemens commissions one of Germany's largest green hydrogen generation plants." siemens. https://press.siemens.com/global/en/pressrelease/siemens-commissions-one-germanys-largest-green-hydrogen-generation-plants (accessed 07 December, 2022).

[9] "Inauguration of the world's largest PEM electrolyzer to produce decarbonized hydrogen." https://www.airliquide.com/stories/industry/inauguration-worlds-largest-pem-electrolyzer-produce-decarbonized-hydrogen (accessed 07 December, 2022).

[10] N. Khelfaoui, A. Djafour, C. Ghenai, I. Laib, M. B. Danoune, and A. Gougui, "Experimental investigation of solar hydrogen production PV/PEM electrolyser performance in the Algerian Sahara regions," *International Journal of Hydrogen Energy,* vol. 46, no. 59, pp. 30524-30538, 2021/08/26/ 2021, doi: https://doi.org/10.1016/j.ijhydene.2020.11.193.

[11] X. Cai, R. Lin, J. Xu, and Y. Lu, "Construction and analysis of photovoltaic directly coupled conditions in PEM electrolyzer," *International Journal of Hydrogen Energy,* vol. 47, no. 10, pp. 6494-6507, 2022/02/01/ 2022, doi: https://doi.org/10.1016/j.ijhydene.2021.12.017.

[12] F. Zhang, B. Wang, Z. Gong, X. Zhang, Z. Qin, and K. Jiao, "Development of photovoltaic-electrolyzer-fuel cell system for hydrogen production and power generation," *Energy,* vol. 263, p. 125566, 2023/01/15/ 2023, doi: https://doi.org/10.1016/j.energy.2022.125566.

[13] J. Kotowicz, Ł. Bartela, D. Węcel, and K. Dubiel, "Hydrogen generator characteristics for storage of renewably-generated energy," *Energy,* vol. 118, pp. 156-171, 2017/01/01/ 2017, doi: https://doi.org/10.1016/j.energy.2016.11.148.

[14] D. Coppitters, W. De Paepe, and F. Contino, "Robust design optimization and stochastic performance analysis of a grid-connected photovoltaic system with battery storage and hydrogen storage," *Energy,* vol. 213, p. 118798, 2020/12/15/ 2020, doi: https://doi.org/10.1016/j.energy.2020.118798.

[15] H. Kojima, K. Nagasawa, N. Todoroki, Y. Ito, T. Matsui, and R. Nakajima, "Influence of renewable energy power fluctuations on water electrolysis for green hydrogen production," *International Journal of Hydrogen Energy,* vol. 48, no. 12, pp. 4572-4593, 2023/02/08/ 2023, doi: https://doi.org/10.1016/j.ijhydene.2022.11.018.

[16] F. N. Khatib *et al.*, "Material degradation of components in polymer electrolyte membrane (PEM) electrolytic cell and mitigation mechanisms: A review," *Renewable and Sustainable Energy Reviews,* vol. 111, pp. 1-14, 2019/09/01/ 2019, doi: https://doi.org/10.1016/j.rser.2019.05.007.
[17] I. A. Razzhivin, M. V. Andreev, and A. V. Kievec, "Increasing the stability of hydrogen production in the wind energy-hydrogen system through the use of synthetic inertia of the wind turbine," *International Journal of Hydrogen Energy,* vol. 47, no. 91, pp. 38495-38505, 2022/11/15/ 2022, doi: https://doi.org/10.1016/j.ijhydene.2022.09.060.
[18] S. H. Frensch, F. Fouda-Onana, G. Serre, D. Thoby, S. S. Araya, and S. K. Kær, "Influence of the operation mode on PEM water electrolysis degradation," *International Journal of Hydrogen Energy,* vol. 44, no. 57, pp. 29889-29898, 2019.
[19] Á. Hernández-Gómez, V. Ramirez, and D. Guilbert, "Investigation of PEM electrolyzer modeling: Electrical domain, efficiency, and specific energy consumption," *International Journal of Hydrogen Energy,* vol. 45, no. 29, pp. 14625-14639, 2020.
[20] J. J. Caparrós Mancera, F. Segura Manzano, J. M. Andújar, F. J. Vivas, and A. J. Calderón, "An optimized balance of plant for a medium-size PEM electrolyzer: design, control and physical implementation," *Electronics,* vol. 9, no. 5, p. 871, 2020.
[21] Y. Honsho, M. Nagayama, J. Matsuda, K. Ito, K. Sasaki, and A. Hayashi, "Durability of PEM water electrolyzer against wind power voltage fluctuation," *Journal of Power Sources,* vol. 564, p. 232826, 2023/04/30/ 2023, doi: https://doi.org/10.1016/j.jpowsour.2023.232826.
[22] V. Papadopoulos, J. Desmet, J. Knockaert, and C. Develder, "Improving the utilization factor of a PEM electrolyzer powered by a 15 MW PV park by combining wind power and battery storage – Feasibility study," *International Journal of Hydrogen Energy,* vol. 43, no. 34, pp. 16468-16478, 2018/08/23/ 2018, doi: https://doi.org/10.1016/j.ijhydene.2018.07.069.
[23] M. A. Hannan *et al.*, "Hydrogen energy storage integrated battery and supercapacitor based hybrid power system: A statistical analysis towards future research directions," *International Journal of Hydrogen Energy,* vol. 47, no. 93, pp. 39523-39548, 2022/12/01/ 2022, doi: https://doi.org/10.1016/j.ijhydene.2022.09.099.
[24] B. Yodwong, D. Guilbert, M. Phattanasak, W. Kaewmanee, M. Hinaje, and G. Vitale, "AC-DC converters for electrolyzer applications: State of the art and future challenges," *Electronics,* vol. 9, no. 6, p. 912, 2020.
[25] F. Parache *et al.*, "Impact of Power Converter Current Ripple on the Degradation of PEM Electrolyzer Performances," *Membranes,* vol. 12, no. 2, p. 109, 2022.
[26] J. Siecker, K. Kusakana, and B. P. Numbi, "Optimal heat recovery during polymer electrolyte membrane electrolysis," *International Journal of Hydrogen Energy,* vol. 47, no. 76, pp. 32692-32706, 2022/09/05/ 2022, doi: https://doi.org/10.1016/j.ijhydene.2022.07.169.
[27] A. Abdollahipour and H. Sayyaadi, "Optimal design of a hybrid power generation system based on integrating PEM fuel cell and PEM electrolyzer as a moderator for micro-renewable energy systems," *Energy,* vol. 260, p. 124944, 2022.
[28] M. Samy, H. I. Elkhouly, and S. Barakat, "Multi-objective optimization of hybrid renewable energy system based on biomass and fuel cells," *International Journal of energy research,* vol. 45, no. 6, pp. 8214-8230, 2021.
[29] S. Impram, S. Varbak Nese, and B. Oral, "Challenges of renewable energy penetration on power system flexibility: A survey," *Energy Strategy Reviews,* vol. 31, p. 100539, 2020/09/01/ 2020, doi: https://doi.org/10.1016/j.esr.2020.100539.

[30] J. Jurasz and A. Beluco, *Complementarity of Variable Renewable Energy Sources*. Academic Press, 2022.

[31] J. Jurasz, F. Canales, A. Kies, M. Guezgouz, and A. Beluco, "A review on the complementarity of renewable energy sources: Concept, metrics, application and future research directions," *Solar Energy,* vol. 195, pp. 703-724, 2020.

[32] Z. Li, W. Zhang, R. Zhang, and H. Sun, "Development of renewable energy multi-energy complementary hydrogen energy system (A Case Study in China): A review," *Energy Exploration & Exploitation,* vol. 38, no. 6, pp. 2099-2127, 2020.

[33] H. Kojima, K. Nagasawa, N. Todoroki, Y. Ito, T. Matsui, and R. Nakajima, "Influence of renewable energy power fluctuations on water electrolysis for green hydrogen production," *International Journal of Hydrogen Energy,* 2022/11/24/ 2022, doi: https://doi.org/10.1016/j.ijhydene.2022.11.018.

[34] M. S. Genç, M. Çelik, and İ. Karasu, "A review on wind energy and wind–hydrogen production in Turkey: A case study of hydrogen production via electrolysis system supplied by wind energy conversion system in Central Anatolian Turkey," *Renewable and Sustainable Energy Reviews,* vol. 16, no. 9, pp. 6631-6646, 2012/12/01/ 2012, doi: https://doi.org/10.1016/j.rser.2012.08.011.

[35] K. Zaik and S. Werle, "Solar and wind energy in Poland as power sources for electrolysis process-A review of studies and experimental methodology," *International Journal of Hydrogen Energy,* 2022.

[36] J. Li, P. Liu, and Z. Li, "Optimal design and techno-economic analysis of a hybrid renewable energy system for off-grid power supply and hydrogen production: A case study of West China," *Chemical Engineering Research and Design,* vol. 177, pp. 604-614, 2022/01/01/ 2022, doi: https://doi.org/10.1016/j.cherd.2021.11.014.

[37] L. Kong, J. Yu, and G. Cai, "Modeling, control and simulation of a photovoltaic/hydrogen/supercapacitor hybrid power generation system for grid-connected applications," *International Journal of Hydrogen Energy,* vol. 44, no. 46, pp. 25129-25144, 2019.

[38] M. Chen, Z. Shen, L. Wang, and G. Zhang, "Intelligent energy scheduling in renewable integrated microgrid with bidirectional electricity-to-hydrogen conversion," *IEEE Transactions on Network Science and Engineering,* vol. 9, no. 4, pp. 2212-2223, 2022.

[39] J. Koponen *et al.*, "Effect of power quality on the design of proton exchange membrane water electrolysis systems," *Applied Energy,* vol. 279, p. 115791, 2020/12/01/ 2020, doi: https://doi.org/10.1016/j.apenergy.2020.115791.

[40] A. Weiß, A. Siebel, M. Bernt, T.-H. Shen, V. Tileli, and H. Gasteiger, "Impact of intermittent operation on lifetime and performance of a PEM water electrolyzer," *Journal of the electrochemical society,* vol. 166, no. 8, p. F487, 2019.

[41] A. Hartig-Weiß, M. Bernt, A. Siebel, and H. A. Gasteiger, "A Platinum Micro-Reference Electrode for Impedance Measurements in a PEM Water Electrolysis Cell," *Journal of The Electrochemical Society,* vol. 168, no. 11, p. 114511, 2021.

[42] X. Guo *et al.*, "Review on Power Electronic Converters for Producing Hydrogen from Renewable Energy Sources," *Dianli Xitong Zidonghua/Automation of Electric Power Systems,* vol. 45, no. 20, pp. 185-199, 2021.

[43] V. Guida, D. Guilbert, G. Vitale, and B. Douine, "Design and Realization of a Stacked Interleaved DC–DC Step-Down Converter for PEM Water Electrolysis with Improved Current Control," *Fuel Cells,* vol. 20, no. 3, pp. 307-315, 2020.

[44] S. Wang *et al.*, "A Semi-Decentralized Control Strategy of a PV-based Microgrid with Battery Energy Storage Systems for Electric Vehicle Charging and Hydrogen Production,"

in *2021 IEEE 4th International Electrical and Energy Conference (CIEEC)*, 28-30 May 2021 2021, pp. 1-6, doi: 10.1109/CIEEC50170.2021.9510719.
[45] X. Gu, Z. Ying, X. Zheng, B. Dou, and G. Cui, "Photovoltaic-based energy system coupled with energy storage for all-day stable PEM electrolytic hydrogen production," *Renewable Energy,* vol. 209, pp. 53-62, 2023/06/01/ 2023, doi: https://doi.org/10.1016/j.renene.2023.03.135.
[46] S. Vudata, Y. Wang, J. M. Fenton, and P. Brooker, "Transient Modeling and Optimization of a PEM Electrolyzer for Solar Photovoltaic Power Smoothing," in *Electrochemical Society Meeting Abstracts 241*, 2022, no. 39: The Electrochemical Society, Inc., pp. 1728-1728.
[47] E. Crespi, G. Guandalini, L. Mastropasqua, S. Campanari, and J. Brouwer, "Experimental and theoretical evaluation of a 60 kW PEM electrolysis system for flexible dynamic operation," *Energy Conversion and Management,* vol. 277, p. 116622, 2023/02/01/ 2023, doi: https://doi.org/10.1016/j.enconman.2022.116622.
[48] R. Ding *et al.*, "Machine learning utilized for the development of proton exchange membrane electrolyzers," *Journal of Power Sources,* vol. 556, p. 232389, 2023/02/01/ 2023, doi: https://doi.org/10.1016/j.jpowsour.2022.232389.
[49] M. E. Günay and N. A. Tapan, "Evaluation of polymer electrolyte membrane electrolysis by explainable machine learning, optimum classification model, and active learning," *Journal of Applied Electrochemistry,* vol. 53, no. 3, pp. 415-433, 2023.
[50] A. Mohamed, H. Ibrahem, and K. Kim, "Machine learning-based simulation for proton exchange membrane electrolyzer cell," *Energy Reports,* vol. 8, pp. 13425-13437, 2022/11/01/ 2022, doi: https://doi.org/10.1016/j.egyr.2022.09.135.
[51] A. Salari, H. Shakibi, A. Habibi, and A. Hakkaki-Fard, "Optimization of a solar-based PEM methanol/water electrolyzer using machine learning and animal-inspired algorithms," *Energy Conversion and Management,* vol. 283, p. 116876, 2023/05/01/ 2023, doi: https://doi.org/10.1016/j.enconman.2023.116876.
[52] T. Hai *et al.*, "-Neural network-based optimization of hydrogen fuel production energy system with proton exchange electrolyzer supported nanomaterial," *Fuel,* vol. 332, p. 125827, 2023/01/15/ 2023, doi: https://doi.org/10.1016/j.fuel.2022.125827.
[53] A. K. Soltani, M. Kandidayeni, L. Boulon, and D. L. St-Pierre, "Modular Energy Systems in Vehicular Applications," *Energy Procedia,* vol. 162, pp. 14-23, 2019/04/01/ 2019, doi: https://doi.org/10.1016/j.egypro.2019.04.003.
[54] X. Li, Z. Shang, F. Peng, L. Li, Y. Zhao, and Z. Liu, "Increment-oriented online power distribution strategy for multi-stack proton exchange membrane fuel cell systems aimed at collaborative performance enhancement," *Journal of Power Sources,* vol. 512, p. 230512, 2021.
[55] T. Wang, Q. Li, X. Wang, W. Chen, E. Breaz, and F. Gao, "A power allocation method for multistack PEMFC system considering fuel cell performance consistency," *IEEE Transactions on Industry Applications,* vol. 56, no. 5, pp. 5340-5351, 2020.
[56] K. Benfriha *et al.*, "Development of an advanced MES for the simulation and optimization of industry 4.0 process," *International Journal for Simulation and Multidisciplinary Design Optimization,* vol. 12, p. 23, 2021.
[57] E. Crespi, G. Guandalini, S. Gößling, and S. Campanari, "Modelling and optimization of a flexible hydrogen-fueled pressurized PEMFC power plant for grid balancing purposes," *International Journal of Hydrogen Energy,* vol. 46, no. 24, pp. 13190-13205, 2021/04/06/ 2021, doi: https://doi.org/10.1016/j.ijhydene.2021.01.085.
[58] A. M. Fernandez, M. Kandidayeni, L. Boulon, and H. Chaoui, "An Adaptive State Machine Based Energy Management Strategy for a Multi-Stack Fuel Cell Hybrid Electric Vehicle,"

IEEE Transactions on Vehicular Technology, vol. 69, no. 1, pp. 220-234, 2020, doi: 10.1109/TVT.2019.2950558.

[59] M. Moghadari, M. Kandidayeni, L. Boulon, and H. Chaoui, "Operating Cost Comparison of a Single-Stack and a Multi-Stack Hybrid Fuel Cell Vehicle Through an Online Hierarchical Strategy," *IEEE Transactions on Vehicular Technology,* pp. 1-13, 2022, doi: 10.1109/TVT.2022.3205879.

[60] A. Khalatbarisoltani, M. Kandidayeni, L. Boulon, and X. Hu, "Power Allocation Strategy Based on Decentralized Convex Optimization in Modular Fuel Cell Systems for Vehicular Applications," *IEEE Transactions on Vehicular Technology,* vol. 69, no. 12, pp. 14563-14574, 2020, doi: 10.1109/TVT.2020.3028089.

[61] C. Dépature, L. Boulon, P. Sicard, and M. Fournier, "Simulation model of a multi-stack fuel cell system," in *2013 15th European Conference on Power Electronics and Applications (EPE)*, 2-6 Sept. 2013 2013, pp. 1-10, doi: 10.1109/EPE.2013.6634727.

[62] N. Marx, L. Boulon, F. Gustin, D. Hissel, and K. Agbossou, "A review of multi-stack and modular fuel cell systems: Interests, application areas and on-going research activities," *International Journal of Hydrogen Energy,* vol. 39, no. 23, pp. 12101-12111, 2014.

[63] Y. Li *et al.*, "Exploration of the configuration and operation rule of the multi-electrolyzers hybrid system of large-scale alkaline water hydrogen production system," *Applied Energy,* vol. 331, p. 120413, 2023/02/01/ 2023, doi: https://doi.org/10.1016/j.apenergy.2022.120413.

[64] J. Parra-Restrepo *et al.*, "Influence of the porous transport layer properties on the mass and charge transfer in a segmented PEM electrolyzer," *International Journal of Hydrogen Energy,* vol. 45, no. 15, pp. 8094-8106, 2020/03/18/ 2020, doi: https://doi.org/10.1016/j.ijhydene.2020.01.100.

[65] P. Cavaliere, "Hydrogen Economy," in *Hydrogen Assisted Direct Reduction of Iron Oxides*: Springer, 2022, pp. 359-387.

[66] Z. Yang, J. Lin, H. Zhang, B. Lin, and G. Lin, "A New Direct Coupling Method for Photovoltaic Module-PEM Electrolyzer Stack for Hydrogen Production," *Fuel Cells,* vol. 18, no. 4, pp. 543-550, 2018.

[67] D. Guilbert and G. Vitale, "Improved hydrogen-production-based power management control of a wind turbine conversion system coupled with multistack proton exchange membrane electrolyzers," *Energies,* vol. 13, no. 5, p. 1239, 2020.

[68] X. Lu *et al.*, "Optimization of power allocation for wind-hydrogen system multi-stack PEM water electrolyzer considering degradation conditions," *International Journal of Hydrogen Energy,* 2022.

[69] F. J. Wirkert, J. Roth, S. Jagalski, P. Neuhaus, U. Rost, and M. Brodmann, "A modular design approach for PEM electrolyser systems with homogeneous operation conditions and highly efficient heat management," *International Journal of Hydrogen Energy,* vol. 45, no. 2, pp. 1226-1235, 2020.

[70] S. M. Alirahmi, E. Assareh, A. Arabkoohsar, H. Yu, S. M. Hosseini, and X. Wang, "Development and multi-criteria optimization of a solar thermal power plant integrated with PEM electrolyzer and thermoelectric generator," *International Journal of Hydrogen Energy,* vol. 47, no. 57, pp. 23919-23934, 2022/07/05/ 2022, doi: https://doi.org/10.1016/j.ijhydene.2022.05.196.

[71] S. M. Alirahmi, S. Rahmani Dabbagh, P. Ahmadi, and S. Wongwises, "Multi-objective design optimization of a multi-generation energy system based on geothermal and solar energy," *Energy Conversion and Management,* vol. 205, p. 112426, 2020/02/01/ 2020, doi: https://doi.org/10.1016/j.enconman.2019.112426.

[72] W. Pirom and A. Srisiriwat, "Experimental Study of Hybrid Photovoltaic-PEM Electrolyzer-PEM Fuel Cell System," in *2022 International Electrical Engineering Congress (iEECON)*, 2022: IEEE, pp. 1-4.

[73] R.-E. Dong, S. Zhanguo, I. B. Mansir, A. M. Abed, and X. Niu, "Energy and exergoeconomic assessments of a renewable hybrid ERC/ORC integrated with solar dryer unit, PEM electrolyzer, and RO desalination subsystem," *Process Safety and Environmental Protection,* vol. 171, pp. 812-833, 2023/03/01/ 2023, doi: https://doi.org/10.1016/j.psep.2023.01.038.

[74] E. Escobedo, D. García, M. Ruiz, A. Izquierdo, D. Pacheco-Catalán, and L. C. Ordóñez, "Design, construction, and performance of a próton exchange membrane water electrolyzer (PEM-WE)," *International Journal of Electrochemical Science,* vol. 18, no. 5, p. 100110, 2023/05/01/ 2023, doi: https://doi.org/10.1016/j.ijoes.2023.100110.

[75] M. Ranjbar Hasani, N. Nedaei, E. Assareh, and S. M. Alirahmi, "Thermo-economic appraisal and operating fluid selection of geothermal-driven ORC configurations integrated with PEM electrolyzer," *Energy,* vol. 262, p. 125550, 2023/01/01/ 2023, doi: https://doi.org/10.1016/j.energy.2022.125550.

[76] W. Sun, L. Feng, A. M. Abed, A. Sharma, and A. Arsalanloo, "Thermoeconomic assessment of a renewable hybrid RO/PEM electrolyzer integrated with Kalina cycle and solar dryer unit using response surface methodology (RSM)," *Energy,* vol. 260, p. 124947, 2022/12/01/ 2022, doi: https://doi.org/10.1016/j.energy.2022.124947.

[77] P. Seyedmatin, S. Karimian, H. Rostamzadeh, and M. Amidpour, "Electricity and hydrogen co-production via scramjet multi-expansion open cooling cycle coupled with a PEM electrolyzer," *Energy,* vol. 199, p. 117364, 2020/05/15/ 2020, doi: https://doi.org/10.1016/j.energy.2020.117364.

[78] F. A. Boyaghchi, M. Chavoshi, and V. Sabeti, "Multi-generation system incorporated with PEM electrolyzer and dual ORC based on biomass gasification waste heat recovery: Exergetic, economic and environmental impact optimizations," *Energy,* vol. 145, pp. 38-51, 2018/02/15/ 2018, doi: https://doi.org/10.1016/j.energy.2017.12.118.

[79] Z. Mohammadi, P. Ahmadi, and M. Ashjaee, "Proposal and multi-criteria optimization of novel biomass-based PEM-DEOFC for generating clean and sustainable power," *Energy,* p. 127352, 2023/04/06/ 2023, doi: https://doi.org/10.1016/j.energy.2023.127352.

[80] B. Ghorbani, S. Zendehboudi, and M. Moradi, "Development of an integrated structure of hydrogen and oxygen liquefaction cycle using wind turbines, Kalina power generation cycle, and electrolyzer," *Energy,* vol. 221, p. 119653, 2021/04/15/ 2021, doi: https://doi.org/10.1016/j.energy.2020.119653.

[81] C. Yilmaz and M. Kanoglu, "Thermodynamic evaluation of geothermal energy powered hydrogen production by PEM water electrolysis," *Energy,* vol. 69, pp. 592-602, 2014/05/01/ 2014, doi: https://doi.org/10.1016/j.energy.2014.03.054.

[82] M. Temiz and I. Dincer, "A unique ocean and solar based multigenerational system with hydrogen production and thermal energy storage for Arctic communities," *Energy,* vol. 239, p. 122126, 2022/01/15/ 2022, doi: https://doi.org/10.1016/j.energy.2021.122126.

[83] I. Holmes-Gentle, S. Tembhurne, C. Suter, and S. Haussener, "Dynamic system modeling of thermally-integrated concentrated PV-electrolysis," *International Journal of Hydrogen Energy,* vol. 46, no. 18, pp. 10666-10681, 2021/03/11/ 2021, doi: https://doi.org/10.1016/j.ijhydene.2020.12.151.

[84] Y. Zhao, Z. Zhu, S. Tang, Y. Guo, and H. Sun, "Electrolyzer array alternate control strategy considering wind power prediction," *Energy Reports,* vol. 8, pp. 223-232, 2022/11/01/ 2022, doi: https://doi.org/10.1016/j.egyr.2022.08.169.

[85] S. Muyeen, R. Takahashi, and J. Tamura, "Electrolyzer switching strategy for hydrogen generation from variable speed wind generator," *Electric Power Systems Research,* vol. 81, no. 5, pp. 1171-1179, 2011.

[86] H. Shakibi *et al.*, "Exergoeconomic and optimization study of a solar and wind-driven plant employing machine learning approaches; a case study of Las Vegas city," *Journal of Cleaner Production,* vol. 385, p. 135529, 2023/01/20/ 2023, doi: https://doi.org/10.1016/j.jclepro.2022.135529.

[87] A. Makhsoos *et al.*, "Design, simulation and experimental evaluation of energy system for an unmanned surface vehicle," *Energy,* vol. 148, pp. 362-372, 2018.

[88] A. Makhsoos, H. Mousazadeh, and S. S. Mohtasebi, "Evaluation of some effective parameters on the energy efficiency of on-board photovoltaic array on an unmanned surface vehicle," *Ships and Offshore Structures,* vol. 14, no. 5, pp. 492-500, 2019.

[89] A. Makhsoos, M. Kandidayeni, L. Boulon, B. G. Pollet, and S. Kelouwani, "Evaluation of High-Efficiency Hydrogen Production from Solar Energy using Artificial Neural Network at the Université du Québec à Trois-Rivières," in *2022 IEEE Vehicle Power and Propulsion Conference (VPPC)*, 1-4 Nov. 2022 2022, pp. 1-6, doi: 10.1109/VPPC55846.2022.10003314.

[90] P. ANUSHKA and R. UPAKA, "Comparison of different artificial neural network (ANN) training algorithms to predict the atmospheric temperature in Tabuk, Saudi Arabia," *Mausam,* vol. 71, no. 2, pp. 233-244, 2020.

[91] Saikesaisi. "Hydrogen and Oxygen Electrolyzer of water electroliser (Qlc-1000 Pem Technology Electrolysis Cell)." Shandong Saikesaisi Hydrogen Energy Co.,Ltd. https://sksshydrogen.en.made-in-china.com/product/QKunFxIovMRm/China-Qlc-1000-Pem-Technology-Electrolysis-Cell.html (accessed.

[92] D. Bessarabov, H. Wang, H. Li, and N. Zhao, *PEM electrolysis for hydrogen production: principles and applications*. CRC press, 2016.

[93] S. Shiva Kumar and V. Himabindu, "Hydrogen production by PEM water electrolysis – A review," *Materials Science for Energy Technologies,* vol. 2, no. 3, pp. 442-454, 2019/12/01/ 2019, doi: https://doi.org/10.1016/j.mset.2019.03.002.

[94] F. Scheepers *et al.*, "Improving the efficiency of PEM electrolyzers through membrane-specific pressure optimization," *Energies,* vol. 13, no. 3, p. 612, 2020.

[95] Á. Hernández-Gómez, V. Ramirez, D. Guilbert, and B. Saldivar, "Cell voltage static-dynamic modeling of a PEM electrolyzer based on adaptive parameters: Development and experimental validation," *Renewable Energy,* vol. 163, pp. 1508-1522, 2021/01/01/ 2021, doi: https://doi.org/10.1016/j.renene.2020.09.106.

[96] D. Falcão and A. Pinto, "A review on PEM electrolyzer modelling: Guidelines for beginners," *Journal of Cleaner Production,* vol. 261, p. 121184, 2020.

[97] B. Yodwong, D. Guilbert, M. Phattanasak, W. Kaewmanee, M. Hinaje, and G. Vitale, "Faraday's efficiency modeling of a proton exchange membrane electrolyzer based on experimental data," *Energies,* vol. 13, no. 18, p. 4792, 2020.

[98] B. Laoun, A. Khellaf, M. W. Naceur, and A. M. Kannan, "Modeling of solar photovoltaic-polymer electrolyte membrane electrolyzer direct coupling for hydrogen generation," *International Journal of Hydrogen Energy,* vol. 41, no. 24, pp. 10120-10135, 2016/06/29/ 2016, doi: https://doi.org/10.1016/j.ijhydene.2016.05.041.

[99] C. Lamy and P. Millet, "A critical review on the definitions used to calculate the energy efficiency coefficients of water electrolysis cells working under near ambient temperature conditions," *Journal of Power Sources,* vol. 447, p. 227350, 2020/01/31/ 2020, doi: https://doi.org/10.1016/j.jpowsour.2019.227350.

[100] G. Papakonstantinou, G. Algara-Siller, D. Teschner, T. Vidaković-Koch, R. Schlögl, and K. Sundmacher, "Degradation study of a proton exchange membrane water electrolyzer under dynamic operation conditions," *Applied Energy,* vol. 280, p. 115911, 2020/12/15/ 2020, doi: https://doi.org/10.1016/j.apenergy.2020.115911.

[101] A. Voronova, H. J. Kim, J. H. Jang, H. Y. Park, and B. Seo, "Effect of low voltage limit on degradation mechanism during high-frequency dynamic load in proton exchange membrane water electrolysis," *International Journal of Energy Research,* vol. 46, no. 9, pp. 11867-11878, 2022.

[102] M. Chandesris, V. Médeau, N. Guillet, S. Chelghoum, D. Thoby, and F. Fouda-Onana, "Membrane degradation in PEM water electrolyzer: Numerical modeling and experimental evidence of the influence of temperature and current density," *International Journal of Hydrogen Energy,* vol. 40, no. 3, pp. 1353-1366, 2015/01/21/ 2015, doi: https://doi.org/10.1016/j.ijhydene.2014.11.111.

[103] E. Kuhnert, M. Heidinger, D. Sandu, V. Hacker, and M. Bodner, "Analysis of PEM Water Electrolyzer Failure Due to Induced Hydrogen Crossover in Catalyst-Coated PFSA Membranes," *Membranes,* vol. 13, no. 3, p. 348, 2023.